A Study of An Oscillating Water Column (OWC) to Harvest Wave Energy Using FLUENT Software

by

MUHAMMAD HAFIZ BIN ROHIMI

Dissertation submitted in partial fulfilment of
the requirement for the
Bachelor of Engineering (Hons)
(Mechanical Engineering)

JULY 2010

Universiti Teknologi PETRONAS

Bandar Seri Iskandar

31750 Tronoh

Perak Darul Ridzuan

CERTIFICATION OF APPROVAL

A Study of An Oscillating Water Column (OWC) to Harvest Wave Energy Using FLUENT Software

by

MUHAMMAD HAFIZ BIN ROHIMI

A project dissertation submitted to the
Mechanical Engineering Programme
Universiti Teknologi PETRONAS
in partial fulfilment of the requirement for the
Bachelor of Engineering (Hons)
(Mechanical Engineering)

Approved:

.....
(Ir. Dr. M. Shiraz Aris)

Project Supervisor

UNIVERSITI TEKNOLOGI PETRONAS

TRONOH, PERAK

DECEMBER 2010

CERTIFICATION OF ORIGINALITY

This is to certify that I am responsible for the work submitted in this project, that the original work is my own except as specified in the references and acknowledgements, and that the original work contained herein have not been undertaken or done by unspecified sources or persons.

.....

MUHAMMAD HAFIZ BIN ROHIMI

ABSTRACT

Oscillating water column (OWC) is the technology for harnessing the motion of ocean or sea waves as they push an air pocket up and down behind a breakwater, turning a turbine and drives a generator to produce electricity. The purpose of this project are to numerically and experimentally study the OWC design, to design and develop an OWC wave generator and investigates its application on offshore structures. The scope of the project is focuses on what is happening inside air chamber where it will involve various types of fluid flow patterns and pressure inside the air chamber. In order to achieve the objectives, Computational Fluid Dynamics (CFD) is used to simulate the flow patterns inside the air chamber. The software used for the CFD analysis are FLUENT and GAMBIT, where the operating conditions and other types of properties can be varied easily to evaluate the flow rate of the air exits and retreat backs to the air chamber and the pressure inside it. Finally, it will lead to design changes that improve the effectiveness of the OWC. There 12 designs of OWC model that have been simulated and studied. The best possible ways to optimize the model are to use 40^{o} of inclined angle or arc radius, increase the height of the entrance inlet, increase the length of the air chamber, reduce the height of the air chamber or change the location of the pipe connected to the air turbine from top to the side of the air chamber. However, since all parameters are connected and related to each other, the best possible design need to be further studies.

ACKNOWLEDGEMENT

Alhamdulillah, thanks to Allah, I managed to complete my final year project within the period given.

First of all, I would like to acknowledge and express my gratitude to my supervisor, Ir. Dr. M. Shiraz Aris for his patience, support, advices, continuous guidance and supervision in helping me during this tough period to complete this project. Not to forget to my Graduate Assistance (GA), Mr. Suren Lim for his support and advices throughout the year.

Lots of thanks also go to my beloved parents, Mr Rohimi bin Yaacob and Mrs Norida binti Yunus, and all family members for their supports in mental, physical and financial aids. Thank you for the time you all spent to share all my tears and laughter.

Last but not least, I would like to express special appreciation and gratitude to all the lecturers, technicians, friends and all who have involved in my final year project. Thank you very much for your understanding, support and cooperation.

A great thankful from me.

TABLE OF CONTENTS

CERTIFICATION OF APPROVAL			ii
CERTIFICATION OF ORIGINALITY			iii
ABSTRACT			iv
ACKNOWLEDGEMENT			v
LIST OF FIGURES			vii
LIST OF TABLES			ix
CHAPTER 1:	**INTRODUCTION**		1
	1.1	Background of Study	1
	1.2	Problem Statement	3
	1.3	Objectives and Scope of Study	4
CHAPTER 2:	**LITERATURE REVIEW**		5
	2.1	Ocean Waves	5
	2.2	OWC	6
	2.3	Harmonic Wave Function	9
CHAPTER 3:	**METHODOLOGY**		10
	3.1	Process Plan	10
	3.2	Project Milestione	11
	3.3	Detailed of the Procedure	11
CHAPTER 4:	**RESULTS AND DISCUSSIONS**		16
	4.1	Results from the Reference Model	16
	4.2	Results from 11 Other Designs	20
	4.3	Discussion	20
CHAPTER 5:	**CONCLUSIONS AND RECOMMENDATIONS**		25
	5.1	Conclusion	25
	5.2	Recommendations	25
REFERENCES			27
APPENDIX A	Project milestone		30
APPENDIX B	Harmonic wave function attached in UDF		31
APPENDIX C	2D design of OWC model		36
APPENDIX D	Contours of dynamic pressure and velocity magnitude (mixture) at 1000 iterations (0.5s flow) for each design		42

LIST OF FIGURES

Figure 1	Groups of wave energy devices.	2
Figure 2	Cut away sketch of a coastal oscillating water column plant .	3
Figure 3	Schematics of the basic principle involved in OWC . .	7
Figure 4	Vertical cross-section of shore-mounted OWC .	7
Figure 5	Project flow	10
Figure 6	2-D drawing of the OWC design (dimension in mm). .	12
Figure 7	Quad-pave face mesh	13
Figure 8	Boundary condition	14
Figure 9	2-D drawing of the OWC design model (reference model) .	15
Figure 10	Scaled residuals until 4000 iterations (2.0s flow) . .	17
Figure 11	Convergence history of dynamic pressure at outflow until 4000 iterations (2.0s flow)	17
Figure 12	Contours of dynamic pressure (left) and velocity magnitude (right) (mixture) for 1000, 2000, 3000 and 4000 iterations . .	18
Figure 13	Flux report	19
Figure 14	Contours of dynamic pressure (mixture) up until 17000iterations (8.5sflow) of design11.	23
Figure 15	Project milestone	30
Figure 16	Constant velocity of function *U(t)*	32
Figure 17	Parabolic function of *U(t,y)*	34
Figure 18	Graph of *y* vs *U(t,y)*	35
Figure 19	2-D drawing of the design0 (reference model) . .	36
Figure 20	2-D drawing of the design1	36
Figure 21	2-D drawing of the design2	37
Figure 22	2-D drawing of the design3	37
Figure 23	2-D drawing of the design4	38
Figure 24	2-D drawing of the design5	38
Figure 25	2-D drawing of the design6	39
Figure 26	2-D drawing of the design7	39
Figure 27	2-D drawing of the design8	40

Figure 28 2-D drawing of the design9 40
Figure 29 2-D drawing of the design10 41
Figure 30 2-D drawing of the design11 41
Figure 31 Contours of dynamic pressure (mixture) of Design1 (0.5s flow) 42
Figure 32 Contours of velocity magnitude (mixture) of Design1 (0.5s flow) 42
Figure 33 Contours of dynamic pressure (mixture) of Design2 (0.5s flow) 43
Figure 34 Contours of velocity magnitude (mixture) of Design2 (0.5s flow) 43
Figure 35 Contours of dynamic pressure (mixture) of Design3 (0.5s flow) 44
Figure 36 Contours of velocity magnitude (mixture) of Design3 (0.5s flow) 44
Figure 37 Contours of dynamic pressure (mixture) of Design4 (0.5s flow) 45
Figure 38 Contours of velocity magnitude (mixture) of Design4 (0.5s flow) 45
Figure 39 Contours of dynamic pressure (mixture) of Design5 (0.5s flow) 46
Figure 40 Contours of velocity magnitude (mixture) of Design5 (0.5s flow) 46
Figure 41 Contours of dynamic pressure (mixture) of Design6 (0.5s flow) 47
Figure 42 Contours of velocity magnitude (mixture) of Design6 (0.5s flow) 47
Figure 43 Contours of dynamic pressure (mixture) of Design7 (0.5s flow) 48
Figure 44 Contours of velocity magnitude (mixture) of Design7 (0.5s flow) 48
Figure 45 Contours of dynamic pressure (mixture) of Design8 (0.5s flow) 49
Figure 46 Contours of velocity magnitude (mixture) of Design8 (0.5s flow) 49
Figure 47 Contours of dynamic pressure (mixture) of Design9 (0.5s flow) 50
Figure 48 Contours of velocity magnitude (mixture) of Design9 (0.5s flow) 50
Figure 49 Contours of dynamic pressure (mixture) of Design10 (0.5s flow) 51
Figure 50 Contours of velocity magnitude (mixture) of Design10 (0.5s flow) 51
Figure 51 Contours of dynamic pressure (mixture) of Design11 (0.5s flow) 52
Figure 52 Contours of velocity magnitude (mixture) of Design11 (0.5s flow) 52

LIST OF TABLES

Table 1	Change of parameters of other 11 design.. . . .	15
Table 2	Wave characteristics in Malaysia	16
Table 3	Dynamic pressure (Pa) and velocity magnitude (m/s) of the mixture at the outlet of each iterations	17
Table 4	Dynamic pressure (Pa) and velocity magnitude (m/s) of mixture for each design at 1000 iterations	20
Table 5	Calculation involved in Microsoft Excel . . .	34

CHAPTER 1
INTRODUCTION

1.1 Background of Study

The enormous energy potential of ocean waves has been recognized throughout history. However, it is only in recent times, following the crisis of the 1970s when attention was focused on the possibility of extracting increased amounts of power from natural energy sources, that the exploitation of ocean waves in the production of electricity was explored in more detail. Experiments on wave energy conversion have indicated that several methods are feasible, and many areas of the world were shown to have the potential coastal wave energy that could be converted into useful power. Several wave energy prototypes have already been deployed worldwide such as in Japan, Norway, India, China, UK and Portugal.

The International Energy Agency (1994a) estimated that wave energy could eventually provide over 10% of the world's current electricity supply. With the exception of tidal waves, generated by earth's rotation within the gravity fields of the sun and the moon, ocean waves appropriate to energy utilization are the product of surface winds. Of significance is that just below the ocean surface the density of wave power is about five times larger than the corresponding wind power 20m above the sea surface, and 20 to 30 times the solar power.

There are various books that discuss behaviour of waves in terms of energy resource and behaviour [1]-[3]. These often go on to discuss the various wave energy devices that are in development. In short, they can be broken down into four basic technology groups [4] & [5]:

- Oscillating Water Column (OWC)

- Overtopping device
- Point Absorbers (floating or mounted on the sea bed)
- Surging devices

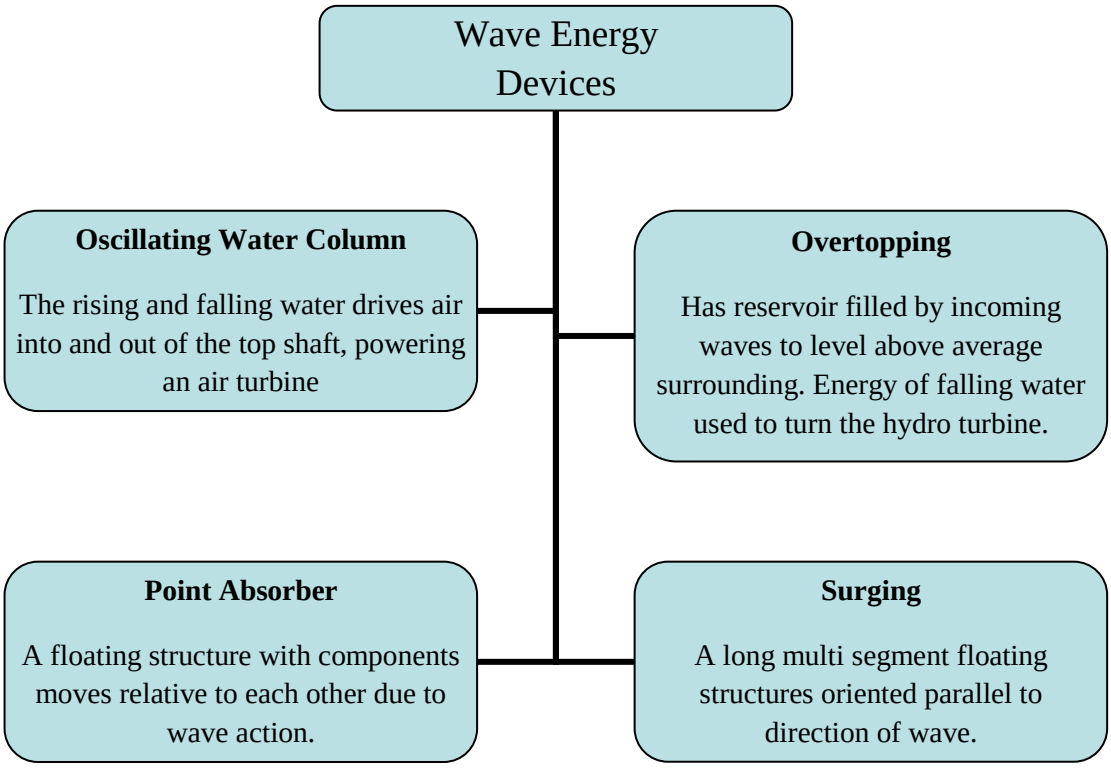

Figure 1: Groups of wave energy devices

The wave generation industry is still debating about the best design and in a recent count there were over 1000 patented ideas for wave energy conversion. For this project, it will simply review shoreline devices which are essentially the oscillating water column type of device. Further detail is discussed in the scope of project section.

OWC generates electricity from the wave-driven rise and fall of water in a cylindrical shaft or pipe. The rising and falling water drives air into and out of the top of the shaft, powering an air-driven turbine. A commonly deployed device is the OWC, which has so far been mounted on shore but is also proposed for floating plants. Incident waves induce a time-varying pressure field inside the device and power is extracted via a turbine and generator. One of the examples of existed OWC is the LIMPET (Land Installed Marine Power Energy Transmitter) in Islay.

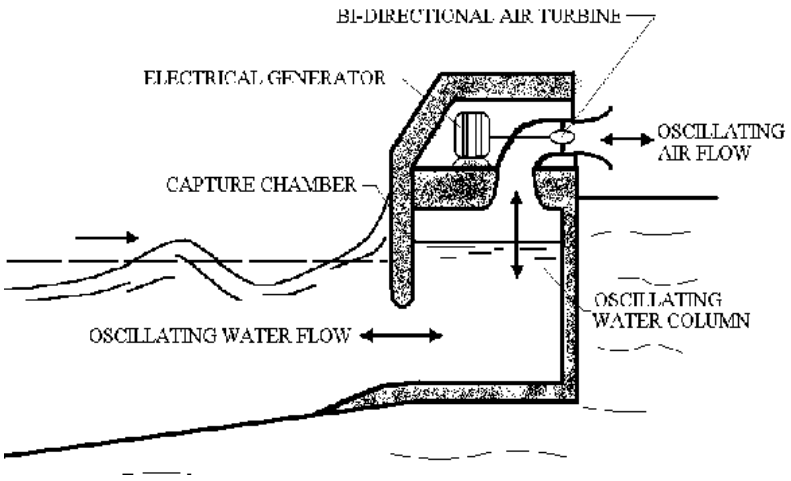

Figure 2: Cut away sketch of a coastal oscillating water column plant

This project is basically focused on the study of this OWC method and it will be further explained in the literature review section.

1.2 Problem Statement

An offshore platform, often referred to as an oil platform or an oil rig, is a large structure used to house workers and machinery needed to drill wells in the ocean bed, extract oil and/or natural gas, process the fluids and ship or pipe them to shore. Offshore oil rigs need electricity to run their machinery and provide a safe, comfortable environment for their workers. Platforms can't very well run cable from land-based power plants if they are miles at sea. So, how do these rigs get the electricity they need? Offshore rigs have generators, most of which are fuelled by diesel oil, to provide the electricity needed on the platforms. Some small, unmanned platforms have solar panels to provide electricity, while a few rigs use natural gas from the wells. [6]

Most rigs use diesel fuel, a petroleum product, which is delivered by tankers. Others use natural gas from the wells; as mentioned before. In particular, parts of the product produced are used to generate them which somehow affect the production target. Thus, wave energy is found to be the perfect alternative renewable energy resources as most offshore platforms are located on the continental shelf, where

wave's growth are constant. This energy is believed can reduce the number of diesel and natural gas usage in providing electricity to the oil rigs. It is suggested to apply the OWC method for usage on offshore oil and gas facilities; specifically, the fixed legs platform. This OWC will be attached to each legs of the platform. However, the OWC method has been used most often for shorelines sites and at some near-shore applications; offshore wave farm is yet to be installed.

1.3 Objectives and Scope of Study

The objectives of this project are:

i. To design and develop an OWC wave generator.

ii. To numerically study the OWC design.

This project will be focuses on the design of the air chamber, apart from the air turbine. The performance of the OWC can be achieved through understanding the air flow within the air chamber to be able to quantify the amount of available energy which can be converted into mechanical energy and subsequently into electricity. A CFD simulation of the air flow into the OWC is expected to assist in optimising the OWC design. Modification will be done to the parameters of the air chamber to see the possible optimisation design. The efficiency of the OWC design will be compared and the most suitable improvement will be selected. Theoretically, the most important part to be focused on the OWC design optimisation is the wall within the air chamber itself as it may plays a big role in affecting the flow rate of the air outflow.

CHAPTER 2

LITERATURE REVIEW

2.1 Ocean Waves

Wave energy can be considered as a concentrated form of solar energy. Winds are generated by the differential heating of the earth and, as they pass over open bodies of water, they transfer some of their energy to form waves. Energy is stored in waves as both potential and kinetic energy. The amount of energy transferred, and hence the size of the resulting waves, depends on the wind speed, the length of time for which the wind blows and the distance over which it blows. Waves lying within or close to the areas where they are generated appear as a complex, irregular wind sea. These waves will continue to travel in the direction of their formation even after the wind is no longer acting on them. In deep water, waves lose energy only slowly, so they can travel out of the storm areas with minimal loss of energy, becoming progressively regular and smooth waves. [7]

Power available in the waves or wave power is the rate of energy transfer per unit area per unit crest width across a plane normal to wave propagation. In deep water, the power in each sea state P is given by:

$$P = 0.5 H_s^{\,2} T_e \text{ kW/m} \qquad (2.1)$$

where H_s is the significant wave height and T_e is the mean wave period with respect to the spectral distribution of wave energy transport. There is tremendous energy in the ocean waves. The total power of waves breaking on the world's coastlines is estimated at 2-3 million megawatts. The west coasts of the United States and Europe and the coasts of Japan and New Zealand are good sites for harnessing wave energy. [8]

Based on Hiroyuki Osawa and Tsuyoshi Miyazaki (2005), for designing of the wave power device, it is necessary to investigate the wave characteristics of the installation sea and to have full understanding of the waves. The principal particulars of the device (size, capacities and so on) have to be decided to convert the wave energy into electricity exhaustively. [9]

Malaysia is a country vastly surrounded by water and its coastline has been divided into four major zones, east peninsular Malaysia, west peninsular Malaysia, Sabah and Sarawak. According to the analysis conducted for the potential of wave energy along the coastline of Malaysia from the data obtained by the Malaysia Meteorological Service (MMS) from 1985 to 2000, locations situated in the South China Sea, especially Terengganu coast has the most promising site for wave power potential. The highest energy resources are available in the months of November to February, which coincide with northeast monsoon season [10]. The total wave energy at Terengganu coast was found to be 17.69 MWh/m in an average year, whereas the average wave power varied between 0.15 to 6.49 kW/m. [11].

2.2 OWC

Since the inception of the UK Wave Energy Performance in 1974, the combination of an OWC collector and a well turbine have been promoted as a reliable and cost effective combination for converting wave energy into useful power [7]. An OWC is formed by a chamber which is filled with air above the water line. Driven by wave action the water level inside the chamber rises and falls, alternately pressurising and rarefying the air within the chamber. As the water level inside the chamber raises pressurised air escapes from the chamber through a turbine-generator unit producing electrical power. As the water level in the chamber falls air is drawn back into the chamber through the turbine-generator assembly to continue power production. Wells turbines are self rectifying so that the direction of the turbine rotation remains constant throughout the power cycle [12]. A generic shore-mounted OWC is shown in cross-section in Figure 3.

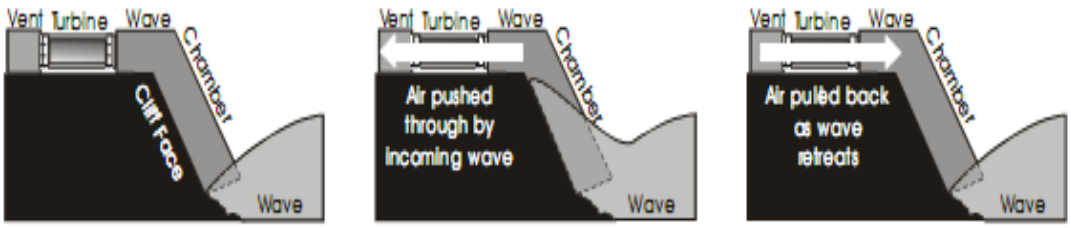

Figure 3: Schematics of the basic principle involved in OWC (*source from http://cfd.bshc.bg/proj_sowatercolumn.htm*)

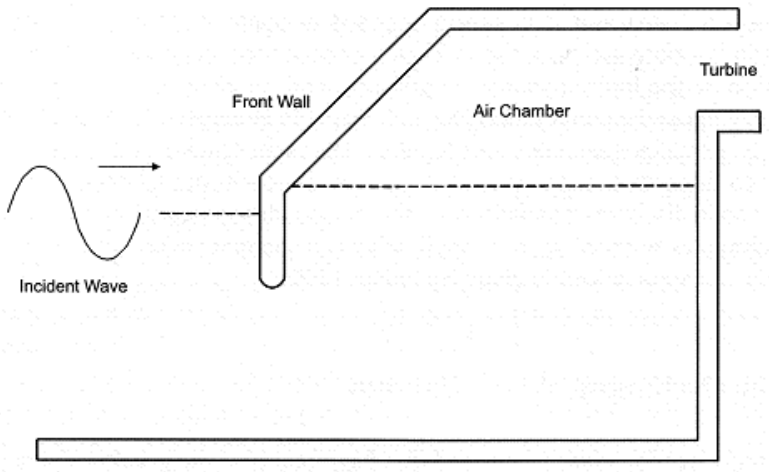

Figure 4: Vertical cross-section of shore-mounted OWC [5]

The shape and thickness of the front wall must ensure that the device survives severe weather conditions, particularly those forces associated with wave slamming. Water flowing past the lip may induce vortex shedding and hence rather turbulent flow within the vicinity of the front wall, though this may be mitigated by a circular lip. As the device is shore-mounted, the incident wave-field is likely to be at best weakly nonlinear and the same remark will apply to the pressure field within the chamber. The forced air-flow within the chamber is unlikely to be smooth or laminar and there is the possibility of water droplets suspended within the air.

Due to Evans (1982), the pressure on the air-water interface is equal to the air pressure p_a and this is taken usually to be constant [12]. With reference to Figure 4, air outside the chamber will be at atmospheric pressure p_a whereas the surface pressure inside the chamber will take a different value and will change due to the

interior conditions in the chamber. If $p_c(t)$ is the air pressure in the chamber, then for harmonic time dependency write

$$p_c(t) = p_a + p(t), \quad p(t) = \mathrm{Re}\{\mathrm{P}e^{-i\omega t}\} \tag{2.2}$$

where p(t) is the difference between the chamber pressure and the external atmospheric pressure. The rate of change of the volume inside the chamber is due to the change in surface level inside the chamber and can be represented as a volume flux Q(t), measured positive in an upwards direction. In linear theory, it can be written as

$$Q(t) = QS(t) + QR(t) = \mathrm{Re}\{(\mathrm{Q}_S + \mathrm{Q}_R)e^{-i\omega t}\} \tag{2.3}$$

associated with the scattered and radiated wave fields respectively.

Based on Paixão Conde and Gato (2008), a typical problem for the OWC system is the design of the air-chamber and the duct, between the water column free-surface (large cross-sectional area and low velocity) and the turbine entrance (small cross-sectional area and high velocity), which requires a sense of balance between safety and efficiency. The air passage should be designed to be as smooth and short as possible, avoiding sudden changes in the flow direction, to prevent poor distribution of the flow at the turbine inlet section, which would seriously reduce the turbine efficiency [13]. A straight vertical connection between the air chamber and the turbine may also raise problems, due to the interaction of the inwards air-jet (from the turbine duct) with the water free-surface, which may produce water-spray that is ingested by the turbine. This may affect the turbine aerodynamic performance and produce severe erosion by droplet impact on the rotor blades [14].

2.3 Harmonic Wave Function

The linear wave theory gives the harmonic wave as its most interesting result. The corresponding analytical expressions for the particle velocities and wave-induced pressure in the water are found with an elegant mathematical technique which is the velocity potential function; a scalar function representing the particle velocities in the water. The use of this function requires the motion of water particles to be irrotational which means, the particle may not rotate around their own axis. The expressions for particle velocities and wave induced pressure are used to find expressions for other wave characteristics, such as phase speed and wave energy.

The particle velocities are given by:

$$u_x = \omega a \frac{\cosh[k(d+z])}{\sinh(kd)} \sin(\omega t - kx) \qquad (2.4)$$

$$u_z = \omega a \frac{\sinh[k(d+z])}{\cosh(kd)} \cos(\omega t - kx) \qquad (2.5)$$

Where,

ω = Radian frequency
a = Amplitude
k = Wave number
z = Height of point submerged from surface
d = Depth to bottom surface

The velocity in y-direction is zero since the long-crested, harmonic wave is propagating in the (positive) x-direction. These velocities are called "orbital velocities" because they are corresponding to motion of the particles in closed, circular or elliptical orbits. [15]

This particle velocity equation is used in writing the sinusoidal function in User Define Function (UDF) in FLUENT to create wave motion as the boundary condition at the inlet is the inlet velocity. Further detail on the UDF is discussed in Appendix B.

CHAPTER 3
METHADOLOGY

3.1 Process Plan

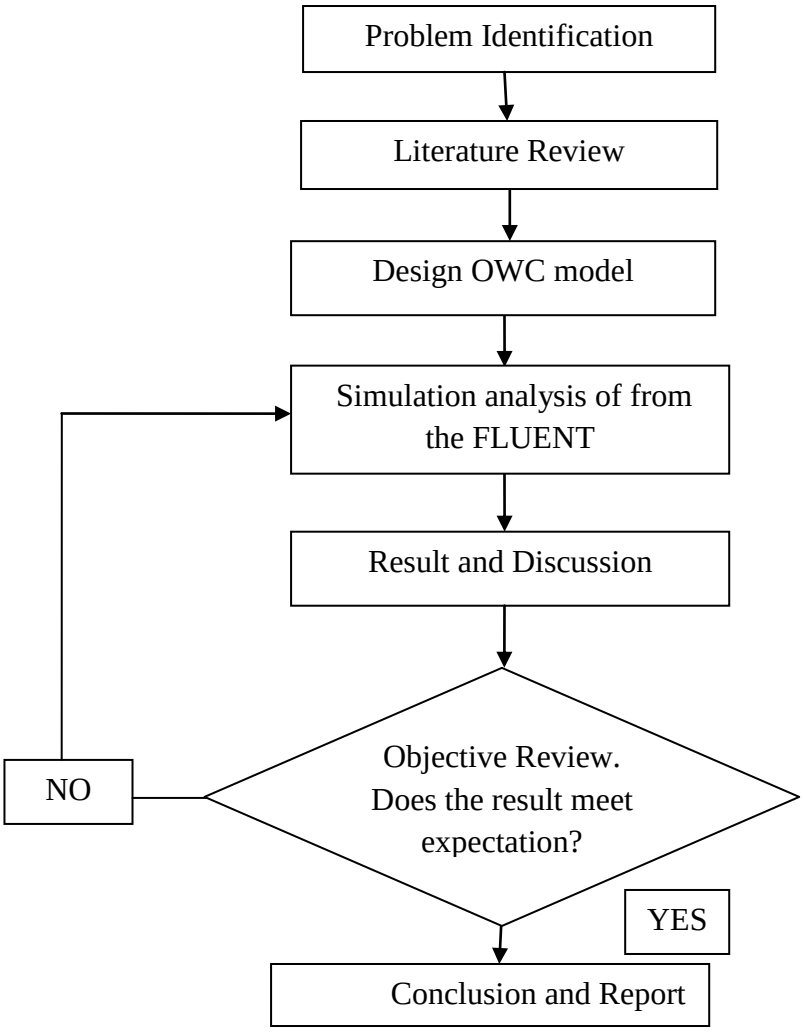

Figure 5: Project Flow

3.2 Project Milestone

Project Milestone of the simulation can be referred to the Appendix A in the Appendices section.

3.3 Detailed of the Procedure

Throughout this project, there are some procedures to be followed to ensure that the project can be accomplished within the given timeframe.

3.2.1 Data research and gathering

Elements of projects involved in this stage include the study of ocean wave characteristics, OWC and its application. Besides that, by referring to the OWC application, the features and types of capture devices are identified.

3.2.2 OWC design

After identified the features and types of capture devices, the best capture device is chose. The design of the OWC is started with sketches and is drawn by using AutoCAD to show it in smaller scale. Figure 6 below shows the drawing of the OWC and its dimension.

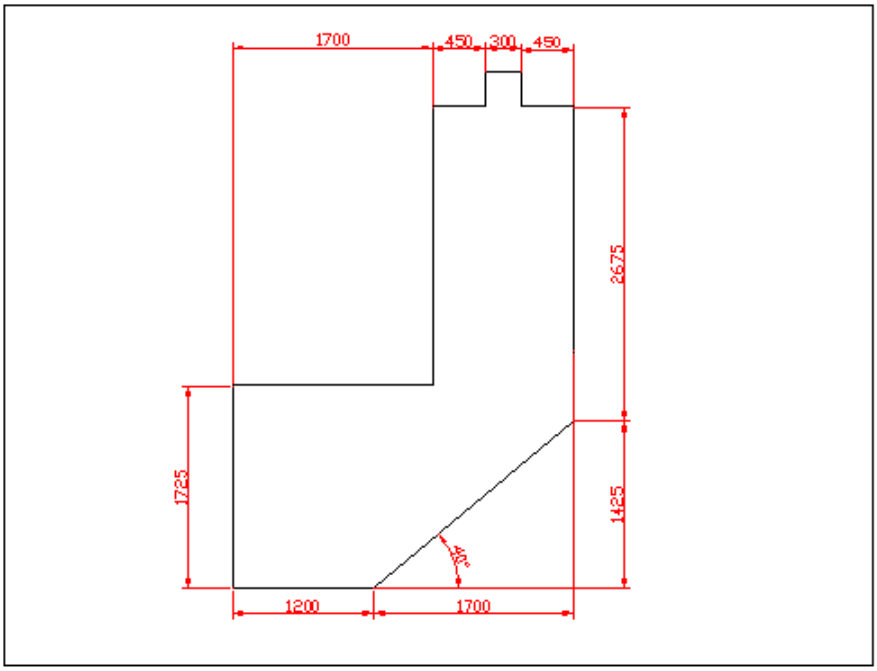

Figure 6: 2-D drawing of the OWC design (*dimension in mm*)

Below are the justifications behind the design of the OWC:

- The front wall of the OWC is decided to be flat vertical and not as the early decision (caisson breakwater), to reduce the loss of the energy from the incoming wave.
- The height of the entrance inlet is big enough to make sure that large volume of ocean water can be sucked into the air chamber so that optimum pressure of air in the air chamber can be achieved.
- The angle or slope between the general parallel front and rear walls to the horizontal is to induce vortex shedding and hence, create the turbulent flow within the air chamber.
- The outlet flow will be connected to a horizontal air turbine such that it has high torque and take shorter time to produce efficient energy from the compressed and decompressed air. [16]

3.2.3 Pre-processing (using GAMBIT)

For the geometry creation of the OWC design, the parameters of the design are selected based on the comparison from the already built LIMPET design; changed to suit the wave height at the Malaysia coast line.

In GAMBIT, the quad face mesh element and pave mesh type are specified as only quadrilateral mesh to be included and to create unstructured grid of mesh elements while the interval size of 0.05 is specified. Therefore, when Quad-Pave meshing scheme is applied, GAMBIT creates an unstructured face mesh consisting of quadrilateral mesh elements as shown in Figure 7.

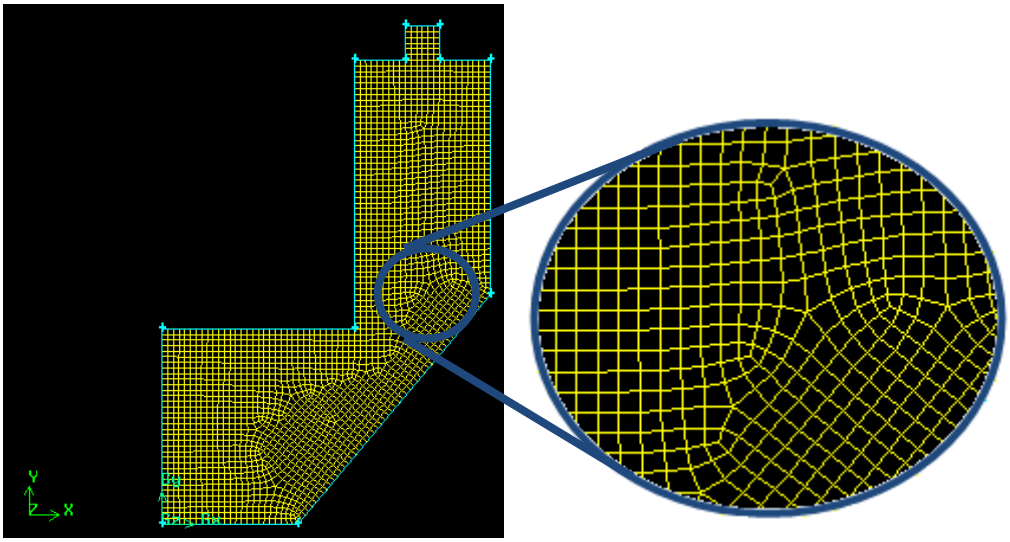

Figure 7: Quad-pave face mesh

The boundary condition of *velocity inlet* is specified at the inlet and *outflow* at the outlet. Other edges of the design are default as *wall*. Figure 8 shows the location of each boundary condition at the OWC design. Fluid continuum type is also specified in GAMBIT.

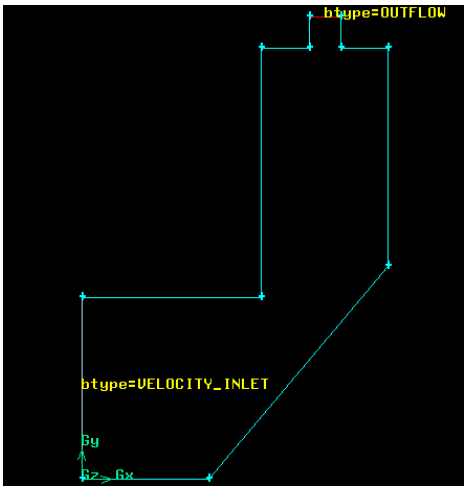

Figure 8: Boundary condition

3.2.4 Solving (using FLUENT)

Numerical model is set up by using the two-dimensional, single precision solver (fluent 2d). The VOF model is used to track the air-water interface and consequently the wave motion. This is followed by selecting an appropriate physical model such as unsteady state as the simulation is time dependent; multiphase, material properties such as water and air are defined, provide sinusoidal motion by using the user define function (UDF) and prescribe the operating condition. The details of function used in UDF can be referred in Appendix B. Boundary conditions which are the velocity inlet and outflow are then assigned. Finally, the solution is computed and monitored.

3.2.5 Post-processing

- The simulation results are examined and interpreted. The dynamic pressure and the velocity magnitude at the outlet is analysed to compare between each designs.
- The best possible optimisation design of the OWC is selected.

3.2.6 Tools and Software

The software used are GAMBIT 2.4.6 and FLUENT 6.3.26.

Figure 9 below shows the 2-D drawing of the OWC design. This design will be the reference as the parameter of the design is changed accordingly to 11other designs which can be seen in the Table 1 below and Appendix C. The parameters used are basically based on estimation to see how much changes will be affected by parameters changed. The changes value of the maximum dynamic pressure at the outlet will be compared and analysed.

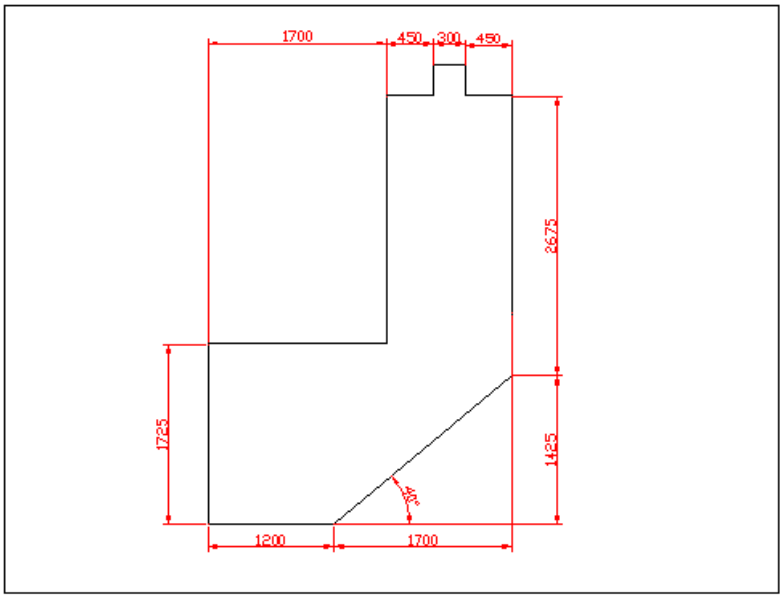

Figure 9: 2-D drawing of the OWC design model (reference model)

Table 1: Change of parameters for other 11 designs

Design	Change of parameters
1	Angle of inclined (50^o)
2	Height of the inlet (2200*mm*)
3	Length of the air chamber (1700*mm*)
4	Height of the air chamber (4600*mm*)
5	Use 2 angle of inclined (40^o)
6	Use 2 angle of inclined (60^o)
7	Angle inclination changed to arc radius (1700*mm* radius)
8	Angle inclination changed to arc radius (2200*mm* radius)
9	Use 2arc radius (700*mm* and 1700*mm* radius)
10	Similar to design 5, but with horizontal outlet
11	Similar to design 6, but with horizontal outlet

CHAPTER 4
RESULTS AND DISCUSSION

There major result that is going to be presented is the simulation part. This section will also include other simulation results that been obtained from the 11other model designs. The maximum dynamic pressure and velocity magnitude at the outlet of each design will be compared and the analysis and justification are discussed in the discussion part.

4.1 Results from the reference model

To analysed and compare the performance of the OWC design, the reference model is first to be studied. For the UDF function, the data gathered of the wave characteristics in Malaysia are used and can be seen at Table 3.

Wave energy	17.69 MWh/m average year
Wave power	0.15-6.49kW/m
Significant wave height	20-120cm
Peak periods	2-8s
Wave number	0.12-0.22rad/m

Table 2: Wave characteristics in Malaysia

Based on table above, the significant wave height which is also the amplitude of 100cm and peak periods of 2s are used. The maximum dynamic pressure is expected to be at quarter of the period cycle which is 0.5s. Therefore, the number of time steps and the time step size use are 1000 and 0.0005s. This means that the simulation are done up until 1000 iterations to get the maximum dynamic pressure in one wave cycle. The simulation is run until 4000 iterations to complete one cycle and the theory is correct, the maximum dynamic pressure is at the quarter of the cycle

(0.5s flow), which is at 1000 iterations. The next maximum dynamic pressure will be obtained on the 5000 iterations; one-quarter of the second cycle (2.5s flow).

Table 3 and Figure 10-12 below show the results when 1000, 2000, 3000 and 4000 iterations are run.

Number of iterations	Max Dynamic Pressure (Pa)	Velocity Magnitude (m/s)
1000	1327.269	48.376
2000	112.190	13.341
3000	1312.778	46.296
4000	117.790	13.674

Table 3: Dynamic pressure (Pa) and velocity magnitude (m/s) of the mixture at the outlet of each iterations

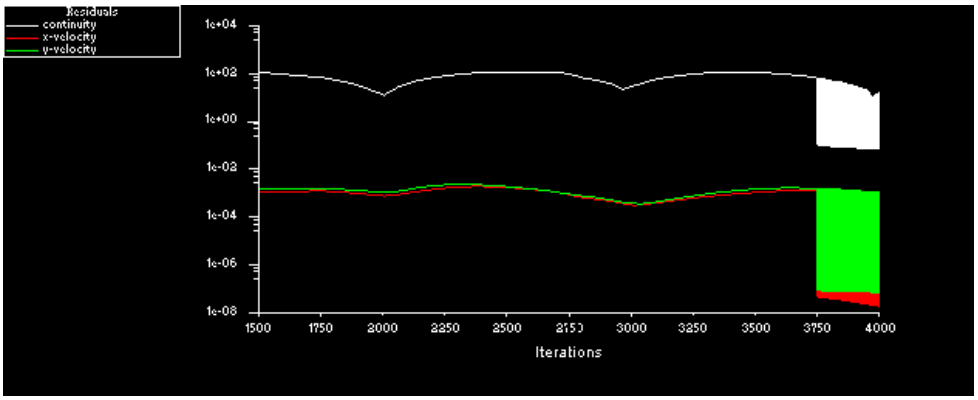

Figure 10: Scaled residuals until 4000 iterations (2.0s flow)

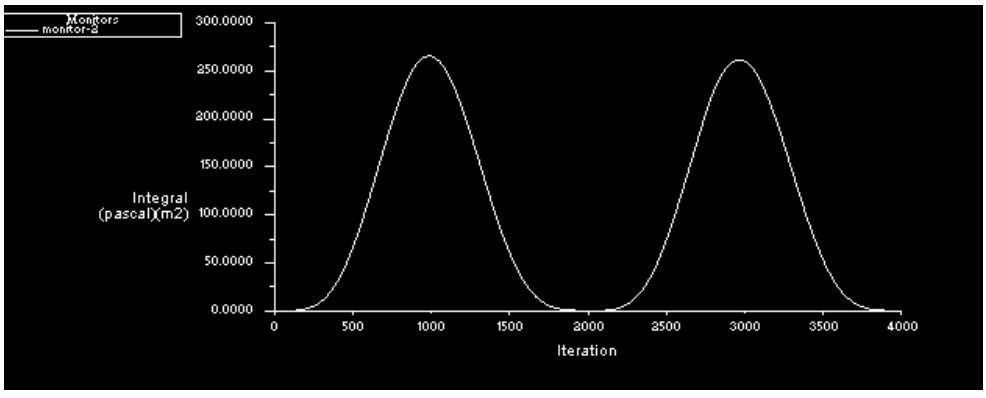

Figure 11: Convergence history of dynamic pressure at outflow until 4000 iterations (2.0s flow)

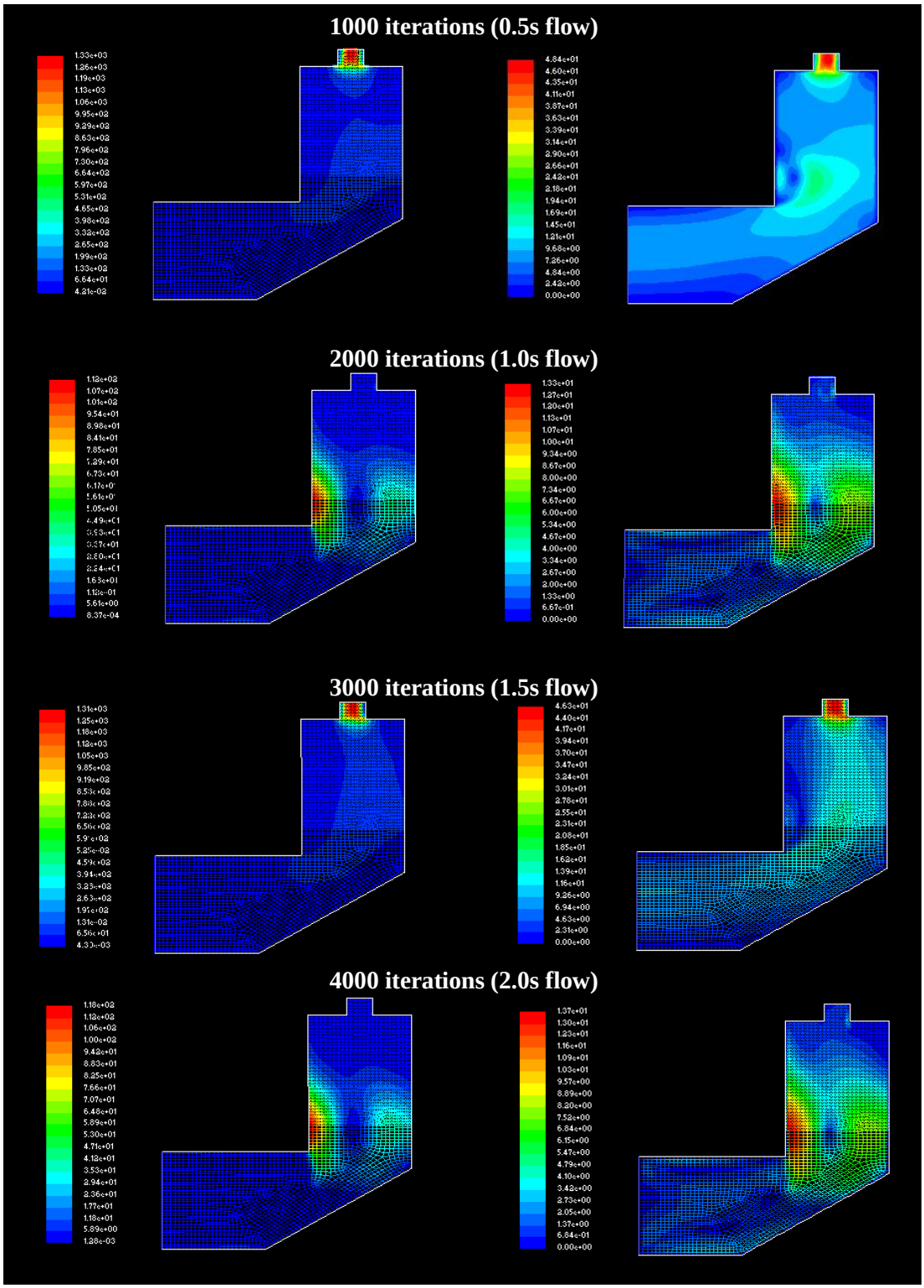

Figure 12: Contours of dynamic pressure (*left*) and velocity magnitude (*right*) (mixture) for 1000, 2000, 3000 and 4000 iterations

From Figure 10, the scaled residuals show that the convergence criterion is in transient flows. From Figure 11, the highest value obtained is at 1000 and 3000 iterations. This result is supported by the contours of dynamic pressure and velocity magnitude in Figure 12, where the maximum values are shown in Table 4 above.

The dynamic pressure is a defined property of a moving flow of gas. Here, the dynamic pressure is applied in a compressible flow. Dynamic pressure is closely related to the kinetic energy of a fluid particle, since both quantities are proportional to the particle's mass (through the density, in the case of dynamic pressure) and square of the velocity.

$$\text{Dynamic pressure, } P_d = \frac{1}{2}\rho V^2$$
$$\text{Kinetic energy, } KE = \frac{1}{2}mV^2 \qquad (4.1)$$

If the value of the dynamic pressure and velocity magnitude from Table 3 are substituted in equation 4.1, the density obtained is 1.225 kg/m^3, which proves the equation above. Dynamic pressure is in fact one of the terms of Bernoulli's equation, which is essentially an equation of energy conservation for a fluid in motion. The dynamic pressure is equal to the difference between the stagnation pressure and the static pressure.

To test whether the simulation is corrected or not, the flux report is obtained and the net mass flow value is approximately near to zero; which means the mass flow at the inlet and the outlet are same; conservation of mass flow.

```
Flow time = 0.5, time step = 1000

zone 7 (default-interior): -142.19563
zone 4 (inlet): 12.969831
zone 5 (outflow): -12.96983
zone 3 (wall): 0
net mass-flow: 9.5367432e-07
```

Figure 13: Flux report

4.2 Results from the 11 other designs

Table 4 below shows the dynamic pressure of the mixture at 1000 iterations for each design. The dynamic pressure and velocity magnitude of design0 at 1000 iterations is referred. The differences of the contours of dynamic pressure and velocity magnitude for each design can be referred at Appendix E.

Design Number	Max Dynamic Pressure (Pa)	Velocity Magnitude (m/s)
0	1327.269	46.551
1	1320.698	46.435
2	1766.092	53.697
3	1359.322	47.109
4	1307.300	46.199
5	1327.756	46.559
6	1335.877	46.701
7	1335.877	48.056
8	1327.817	46.560
9	1421.238	48.170
10	1357.412	48.689
11	1452.036	47.076

Table 4: Dynamic pressure (Pa) and velocity magnitude (m/s) of mixture for each design at 1000 iterations

Based on the table above, it shows that the highest dynamic pressure and velocity magnitude obtained is from the design2 which is by changing the height of the inlet. This was followed by the design11 and design9. All of the analysis will be discussed in the discussion part below.

4.3 Discussion

The difference between the design1 and design0 (reference model) is the inclined angle which changed from 40^{o} to 50^{o}. From the results, the dynamic pressure of

design1 is lower than the design0. As the inclined angle is increasing, it is predicted that the dynamic pressure will decrease. Therefore, it can be said that 40^{o} of inclined angle is suitable enough to induce vortex shedding and hence, create the turbulent flow within the air chamber.

As for design2, the height of the entrance is increased from 1.725m to 2.20m. The dynamic pressure obtained from design2 is the largest one compared to other design. By increasing the height of the inlet, larger volume of ocean water can be sucked into the air chamber so that optimum pressure of air in the air chamber can be achieved. However, the best possible height of the entrance inlet could not be stated as further input data should be studied.

The length of the air chamber is changed from 1.2m to 1.7m for the design3. By doing this, the dynamic pressure obtained is higher than from the design0. Larger volume of air can be compressed here and this affected the dynamic pressure at the outlet, as well as the velocity magnitude. In other words, the work done from the volume changes is increasing by increasing the length of the air chamber.

As for design4, the height of the air chamber is increased from 4.1m to 4.6m; resulting the dynamic pressure lower compared to the reference model. This concept is the same applied to the pipeline. As the pipeline goes longer, the pressure drop will be larger.

In design5, another inclined angle of 40^{o} to the design is added. The same thing goes to design6, where the angle is changed from 40^{o} to 60^{o}. Based on the results, both design gave larger dynamic pressure; design6 produce larger dynamic pressure than design5. By replacing the edge of 90^{o} to an inclined angle, it will reduce the energy loss of wave due to the impact at the outer surface and also inside the air chamber itself.

For design7 and design8, the inclined angle of 40^{o} is changed to a respective arc radius of 1.7m and 2.2m. Both design produce larger dynamic pressure than the reference model; with design7 is more efficient than design8. By changing the incline angle to a respective arc radius surface which is a smoother surface, it will reduce the energy loss of wave due to the impact inside the air chamber.

For design9, a 0.7m arc radius is added to replace the 90^o edge. The result shows the dynamic pressure obtained is larger than the reference model. Design9 gave better result at the arc radius surface provide a smoother surface for the wave impact, compared to desgin5.

As for design10 and design11, the location of the pipe connected to the air turbine is changed from the top location to the side of the air chamber; compared with design 5 and 6. From here, it is found that the best possible location of the pipe connected to the air turbine is at the side of the air chamber. A straight vertical connection between the air chamber and the turbine may also raise problems, due to the interaction of the inwards air-jet (from the turbine duct) with the water free-surface, which may produce water-spray that is ingested by the turbine. This may affect the turbine aerodynamic performance and produce severe erosion by droplet impact on the rotor blades.

Even though design2 gave the highest dynamic pressure, it does not mean that it is the best design. From all the designs, design11 is ought to be the best design as it not only gave the second highest dynamic pressure due to both 40^o inclined angle surface and horizontal connection from the air chamber to the turbine (safety reason). Therefore, further iterations have been done to see the result of other flow time and to see the effect of difference of water level. Figure 14 below shows the result up until 17000 iterations for design11.

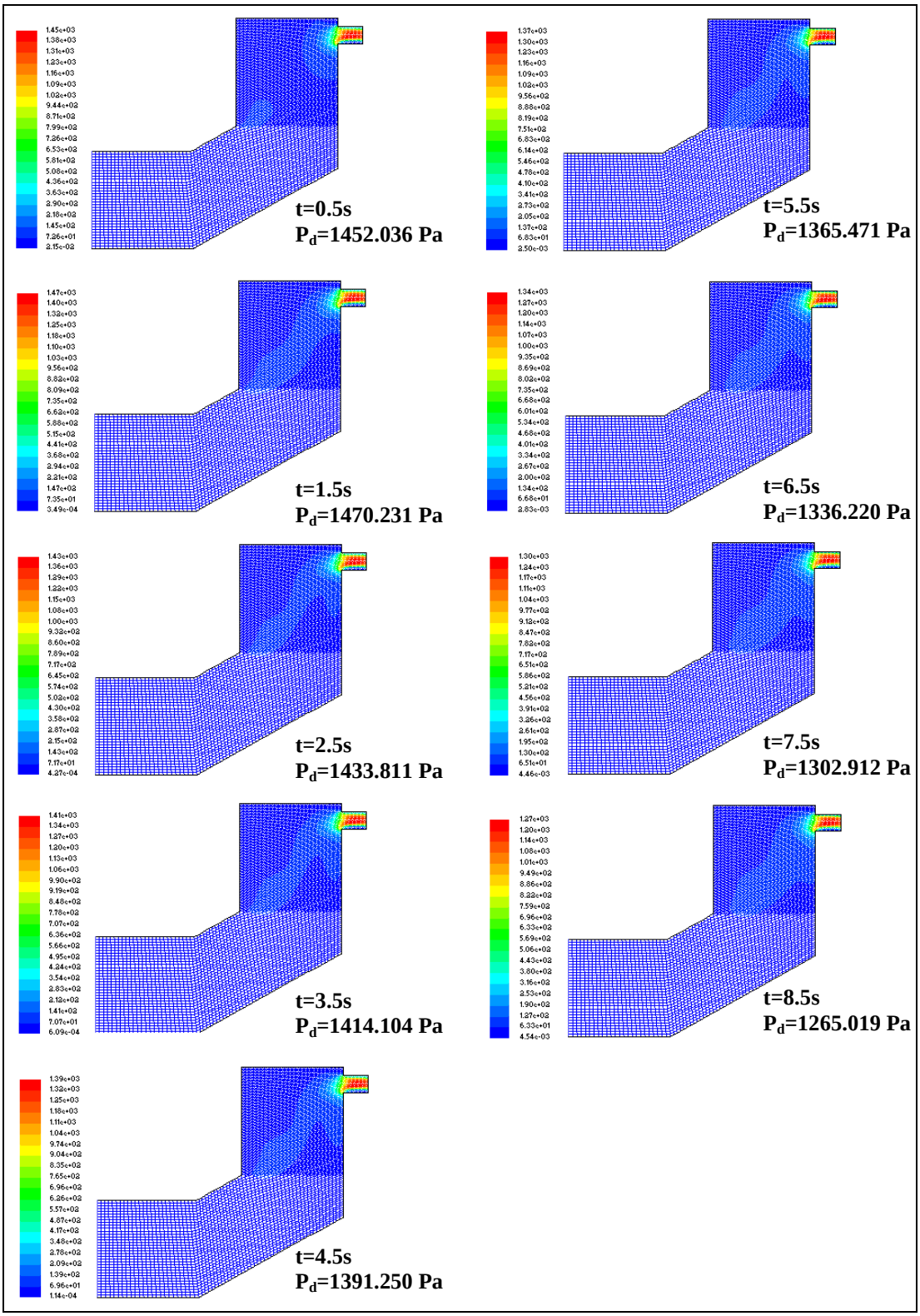

Figure 14: Contours of dynamic pressure (mixture) up until 17000iterations (8.5s flow) of design11

Based on Figure 14, the dynamic pressure is increasing and reaches the maximum at 3000 iterations (1.5s flow). It then started to decrease afterwards until 17000 iterations (8.5s flow) as the iterations stopped at 17998 and updating. The difference of the water level in the air chamber could not be seen as the changes are very small. This is due to the equation used in the UDF function where it is based on the small-amplitude approximation; the amplitude of the horizontal velocity is constant over the vertical.

The work done can be found by applying the ideal gas law. By assuming that the temperature in the air chamber does not change (isothermal process), the work done by the pressurized air due to the changes of water level in the air chamber can be found by using the equation below.

$$P_1V_1 = P_2V_2 = nRT \tag{4.1}$$

$$W_{done} = PV \ln \frac{V_f}{V_o} \tag{4.2}$$

However, as the difference of the water level is small, the changes of the volume could not be calculated.

CHAPTER 5
CONCLUSION AND RECOMMENDATIONS

5.1 Conclusion

In order to improve the existing design system of the OWC such that it can be applied and installed at the offshore structures, lots of research and studies are required to get better understanding on how does the system works. In a way to improve the OWC performance, it can be achieved by understanding what exactly happens inside the air chamber; apart the design of the air turbines. A CFD simulation of the air flow into the OWC column is expected to assist in optimising the OWC design.

Based on the result from the simulation, the best possible ways to optimize the model are:

- Use 40^{o} of inclined angle or arc radius
- Increase the height of the entrance inlet
- Increase the length of the air chamber
- Reduce the height of the air chamber
- Relocate the pipe connecting the air chamber to the air turbine; horizontal connection.

However, since all parameters are connected and related to each other, the best possible design needs to be studies further.

5.2 Recommendations

There are so many factors that affect the efficiency of the OWC model. For a better simulation, it is recommended to use a 3-D simulation as more vary design can be studied such as orifice or spiral wall and cylindrical or square shape design. Besides,

the effect of the width of the OWC model related to its height and length also can be studied.

Besides that, as it is recommended to simulate a 3-D model, thus, both particle velocity equation U_x and U_z should be used. However, it is suggested to find other wave equations to provide wave motion in the FLUENT as the equation used now in the simulation is based on the small-amplitude approximation; thus the water level changes in the air chamber are small.

For the meshing section, mesh refinement, mesh type and size should be rechecked. Further value of mesh size and different mesh types should used to find the best result of the simulation.

REFERENCES

[1] M.J. Tucker and E.G. Pitt, *Waves in Ocean Engineering*, Elsevier Publishers, Ocean Engineering Series, 2001.

[2] R. Shaw, *Wave Energy: A design challenge*, Ellis Horwood Publishers, 1982.

[3] M. E. McCornick, *Ocean Energy conversion*, John Wiley & Sons Publishers, New York, 1981.

[4] A. Clement, P. McCullen, A. Falcao, A. Fiorentino, F. Gardner, K. Hammarlund, G. Lemonis, T. Lewis, K. Nielsen, S. Petroncini, M.-T. Pontes, P. Schild, B.-O. Sjostrom, H.C. Sorensenaan and T. Thorpe., "*Wave Energy in Europe: current status and perspectives", Renewable and Sustainable Energy Reviews* Vol. 6, Elsevier Science Publishers, pp 405-431, 2002.

[5] J. R. Halliday and D. G. Dorrel, "Review of Wave Energy Resource and Wave generator Developments in the UK and the Rest of the World", *IASTED EuroPES conference*, Rhodes, Greece, 28-30 June 2004 (on CD).

[6] How do the offshore oil rigs get the electricity? - http://www.docstoc.com/docs/633582/SECONDARY-ARTICLE-Offshore-Wind- Energy-Offshore-oil-rigs/

[7] R. Bhattacharyya & M.E. McCormick, Elsevier Ocean Engineering Book Series (Volume 6): Wave Energy Conversion, 2003, Elsevier.

[8] Minerals Management Service, U.S. Department of the Interior, *Ocean Energy*, National Energy Education Development (NEED) Project.

[9] Hiroyuki Osawa, Tsuyoshi Mizayaki, *Technical Manual for Oscillating Water Column Type Wave Power Device*, Japan Agency for Marine-Earth Science and Technology (JAMSTEC), The International Society of Offshore and Polar Engineers, Yokosuka, Kanagawa, Japan, 2005.

[10] E.P. Chiang, Z.A. Zainal, P.A. Aswatha Narayana and K.N. Seetharamu, *Potential of Renewable Wave and Offshore Wind Energy Sources in Malaysia*, School of Mechanical Engineering, Pulau Pinang, Malaysia, 2000.

[11] Muzathik AM, Wan Nik WB, Ibrahim MZ, Samo KB, *Ocean Wave Energy Along Terengganu Coast of Malaysia*, University Malaysia Terengganu, Kuala Terengganu, Malaysia, 2009.

[12] João Cruz, *Ocean Wave Energy: Current Status and Future Perspectives*, Springer-Verlag Berlin Heidelberg, 2008.

[13] Folley M, Curran R, Whittaker T, Comparison of LIMPET contra-rotating Wells turbine with theoretical and model test predictions, Ocean Eng 2006, 33:1056-69.

[14] Martins E, Ramos FS, Carrilho L, Justino PAP, Gato LMC, Trigo L, et al. CEODOURO project: overall design of an OWC in the new Oporto breakwater, In: Proceedings of the sixth European wave tidal Energy conference, Glasgow, UK, 2005.

[15] Leo H. Holthuijsen, Waves in Oceanic and Coastal Waters, Cambridge University Press, United Kingdom, 2007.

APPENDICES

APPENDIX A – Project milestone

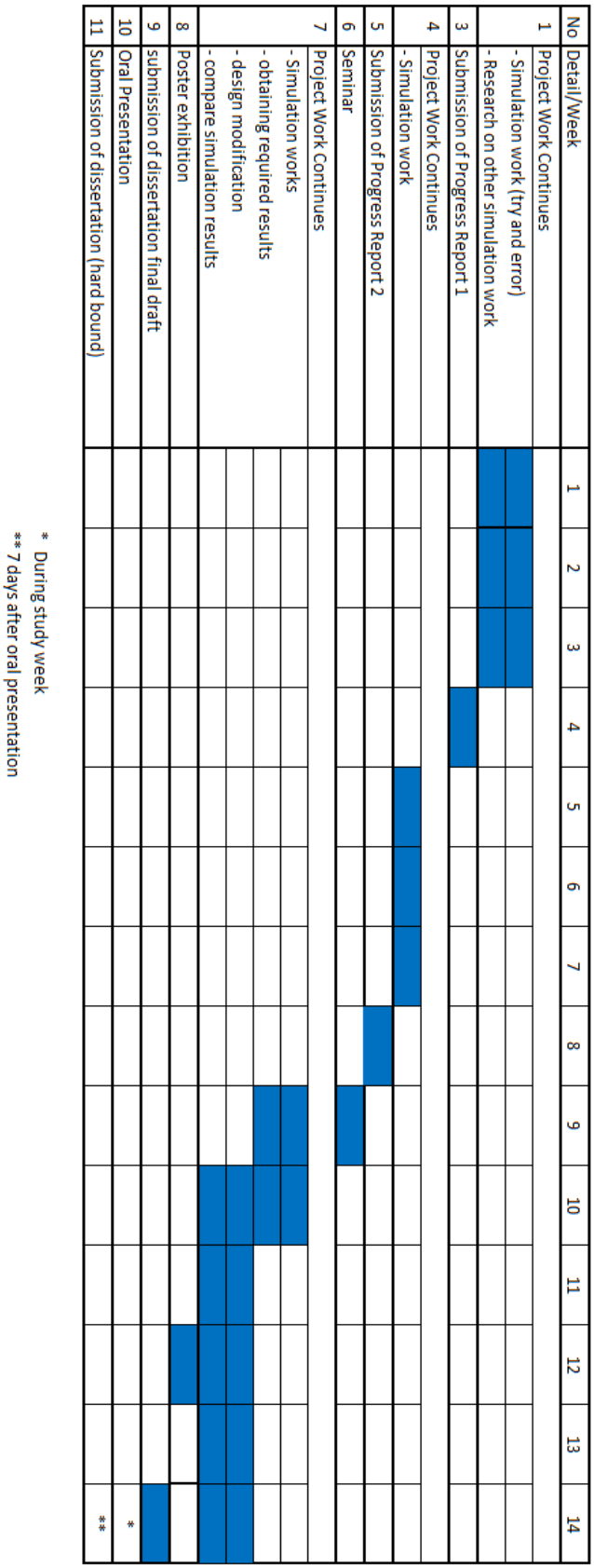

Figure 15: Project milestone

APPENDIX B – Harmonic wave function attached in UDF

```
#include "udf.h"
DEFINE_PROFILE(vel_x_sin, thread, i)
{       real Y[ND_ND];
        real y;
        face_t f;
        real t = CURRENT_TIME;

        real omega;
        real a;
        real k;
        real d;
        real h;

        omega = 3.174;
        k = 0.22;
        d = 10;
        a = 1;
        h = 1.725;

                begin_f_loop(f, thread)
                {       F_CENTROID(Y, f, thread);
                        y = Y[1];

                        F_PROFILE(f, thread, i) = (omega*a*(exp(k*(7.825+y)) +
exp(-k*(7.825+y)))*sin(omega*t)/(exp(k*d) - exp(-k*d)))*(-
6*y*y*(omega*a*(exp(k*(7.825+y)) + exp(-k*(7.825+y)))*sin(omega*t)/(exp(k*d)
- exp(-k*d)))/(h*h)+6*y*(omega*a*(exp(k*(7.825+y)) + exp(-
k*(7.825+y)))*sin(omega*t)/(exp(k*d) - exp(-k*d)))/h);
                }
                end_f_loop(f, t)
}
```

Below is the particle velocity equation as discussed from the literature review part.

$$U(t) = \omega a \frac{\cosh[k(d+z)]}{\sinh(kd)} \sin(\omega t - kx) \\ = \omega a \frac{\cosh[k(d+z)]}{\sinh(kd)} \sin(\omega t) \quad (2.4)$$

kx in the equation 2.4 above is neglected as *x*-position is fixed. The function *U(t)* above is constant at every point and can be shown in Figure 16 below.

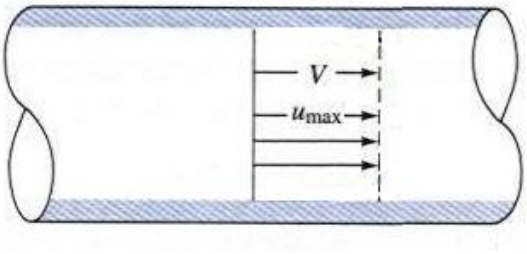

Figure 16: Constant velocity of function *U(t)*

In order to make it in parabolic motion, it is assumed that the function *U(t)* will be in parabolic when it times with a parabolic equation of *U(y)*. Below are the steps involved in deriving the function *U(t,y).*

Assumption:

$$U(y) = Ay^2 + By + C$$

$$U(0) = 0$$
$$U(h) = 0$$
$$U(\frac{h}{2}) = U_{max}$$
$$\therefore U(y) = -\frac{4U_{max}}{h^2} y^2 + \frac{4U_{max}}{h} y$$

$$\int_0^h U(y)dy = \int_0^h \left(-\frac{4U_{max}}{h^2} y^2 + \frac{4U_{max}}{h} y \right) dy$$
$$= -\frac{4U_{max}}{3h^2} y^3 + \frac{4U_{max}}{2h} y^2 \Big|_0^h$$
$$= -\frac{4}{3} U_{max} h + 2U_{max} h$$
$$= \frac{2}{3} U_{max} h$$

By using volumetric flow rate:

$$\int_0^h U_{avg}\,dy = U_{avg}.h$$

$$U_{avg}.h = \frac{2}{3}U_{\max}h$$

$$U_{\max} = \frac{3}{2}U_{avg}$$

Substitute $U_{\max}$ in $U(y)$

$$U(y) = -\frac{4U_{\max}}{h^2}y^2 + \frac{4U_{\max}}{h}y$$

$$= -\frac{4y^2}{h^2}\left(\frac{3}{2}U_{avg}\right) + \frac{4y}{h}\left(\frac{3}{2}U_{avg}\right)$$

$$= -6\frac{y^2}{h^2}U_{avg} + 6\frac{y}{h}U_{avg}$$

$$U(t) = U_{avg}$$

Therefore,

$$U(t,y) = U(t).U(y)$$

$$= \left[\omega a\frac{\cosh[k(d+z)]}{\sinh(kd)}\sin(\omega t)\right]\left[-\frac{6y^2}{h^2}U_{avg} + \frac{6y}{h}U_{avg}\right]$$

$$= \left[\omega a\frac{\cosh[k(d+z)]}{\sinh(kd)}\sin(\omega t)\right]\left[-\frac{6y^2}{h^2}U_{avg} + \frac{6y}{h}U_{avg}\right]$$

$$= \left[\omega a\frac{e^{k(7.825+y)} + e^{-k(7.825+y)}}{e^{kd} - e^{-kd}}\sin(\omega t)\right]\left[-\frac{6y^2}{h^2}U_{avg} + \frac{6y}{h}U_{avg}\right]$$

where

Radian frequency, $\omega = 3.174$

Wave number, $k = 0.22$

Depth to bottom surface, $d = 10$

Amplitude, $a = 1$

Opening of the inlet, $h = 1.725$

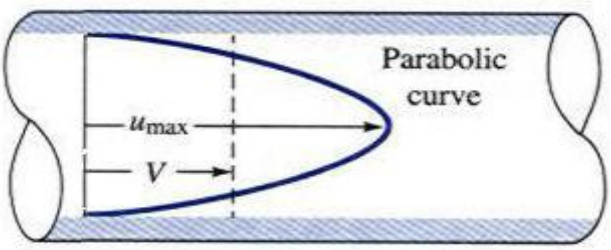

Figure 17: Parabolic function of *U(t,y)*

Table 5: Calculation involved in Microsoft Excel

y	***U(t)*, where *t = 0.5s***	***U(y)***	***U(t).U(y)***
0.000	2.05481	0.00000	0.00000
0.100	2.09771	0.68734	1.44185
0.200	2.14164	1.31710	2.82075
0.300	2.18659	1.88485	4.12140
0.400	2.23261	2.38595	5.32690
0.500	2.27971	2.81552	6.41855
0.600	2.32791	3.16842	7.37578
0.700	2.37723	3.43927	8.17595
0.800	2.42771	3.62244	8.79424
0.863	2.45985	3.68978	9.07632
0.900	2.47936	3.71201	9.20343
1.000	2.53222	3.70179	9.37373
1.100	2.58629	3.58528	9.27260
1.200	2.64162	3.35571	8.86452
1.300	2.69823	3.00597	8.11080
1.400	2.75615	2.52864	6.96930
1.500	2.81540	1.91596	5.39418
1.600	2.87601	1.15983	3.33567
1.700	2.93801	0.25178	0.73972
1.725	2.95373	0.00000	0.00000

Graph of *U(t,y)* vs *y* is plotted, as shown in Figure 18. From the graph, it shows that the velocity is in parabolic motion according to height of the points.

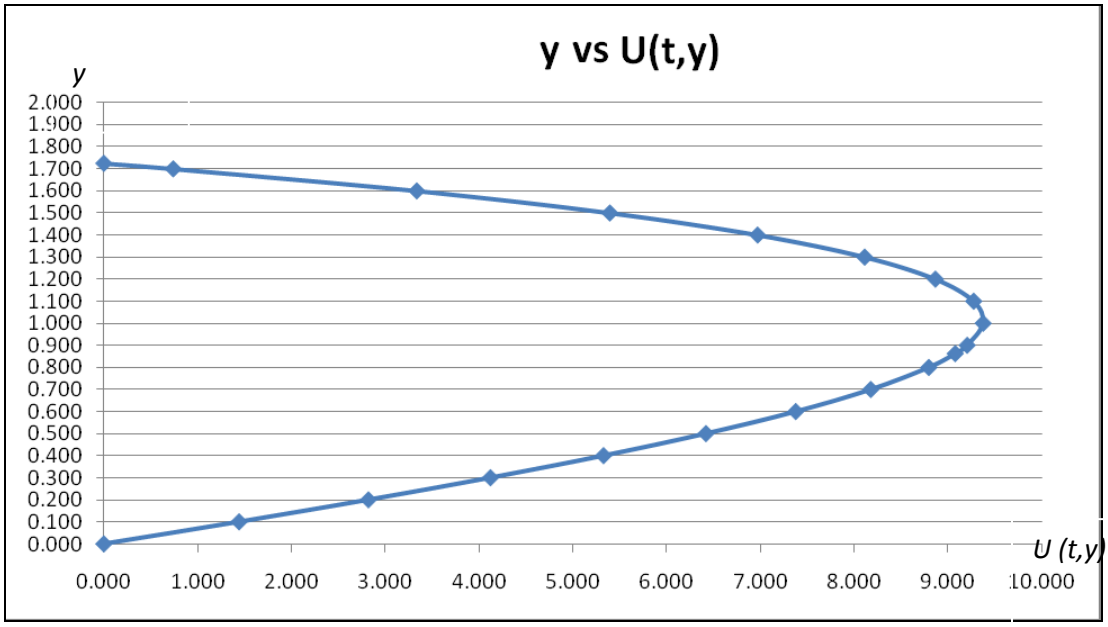

Figure 18: Graph of *y* vs *U(t,y)*

APPENDIX C – 2D design of OWC model

1) Design0 (reference model)

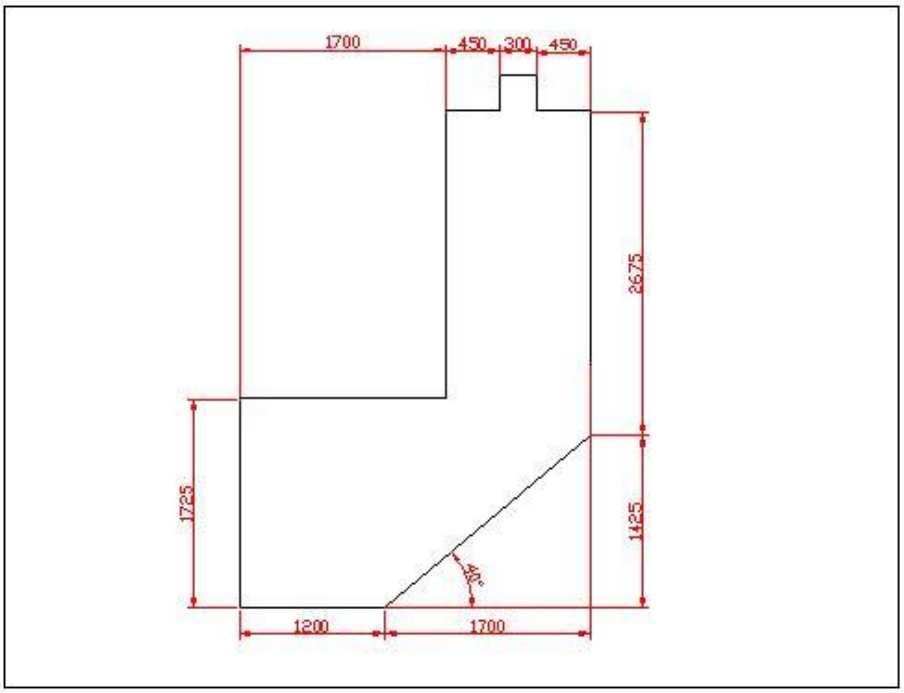

Figure 19: 2-D drawing of the design0 (reference model)

2) Design1 - Angle of inclined (50^{o})

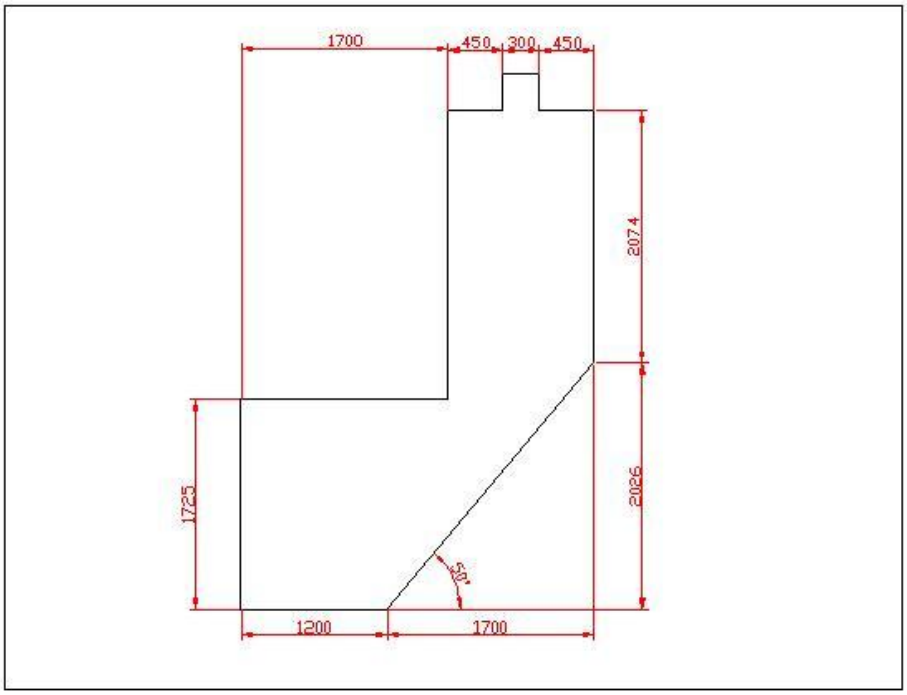

Figure 20: 2-D drawing of the design1

3) Design2 - Height of the entrance inlet (2200*mm*)

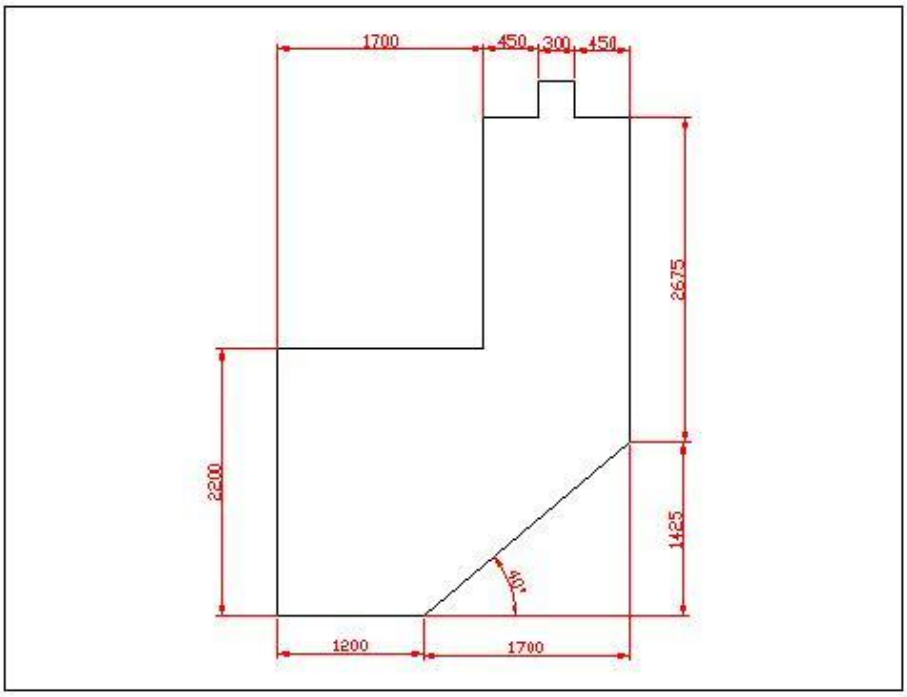

Figure 21: 2-D drawing of the design2

4) Design3 - Length of the air chamber (1700*mm*)

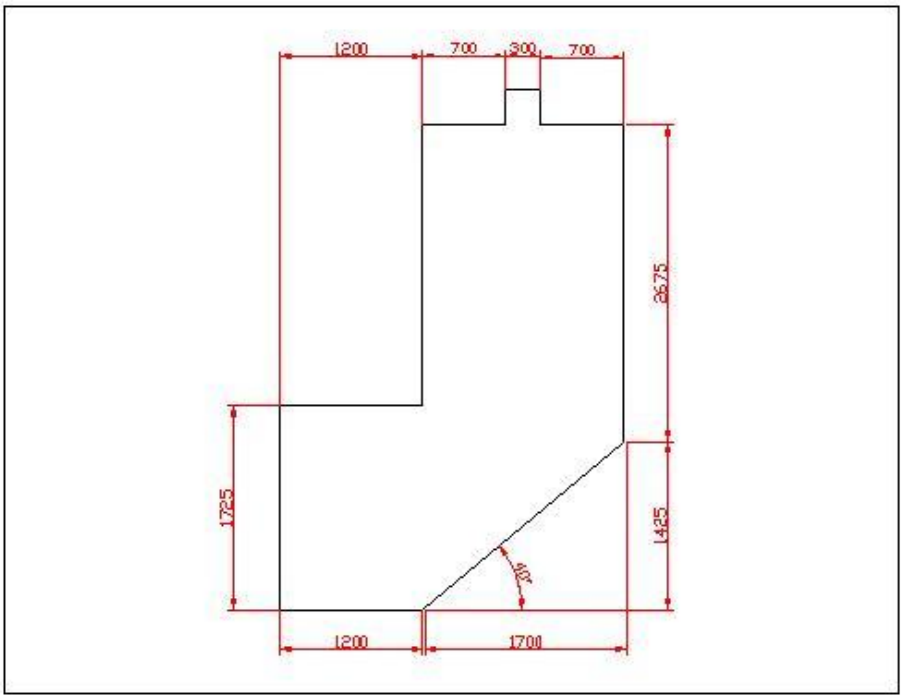

Figure 22: 2-D drawing of the design3

5) Design4 - Height of the air chamber (4600*mm*)

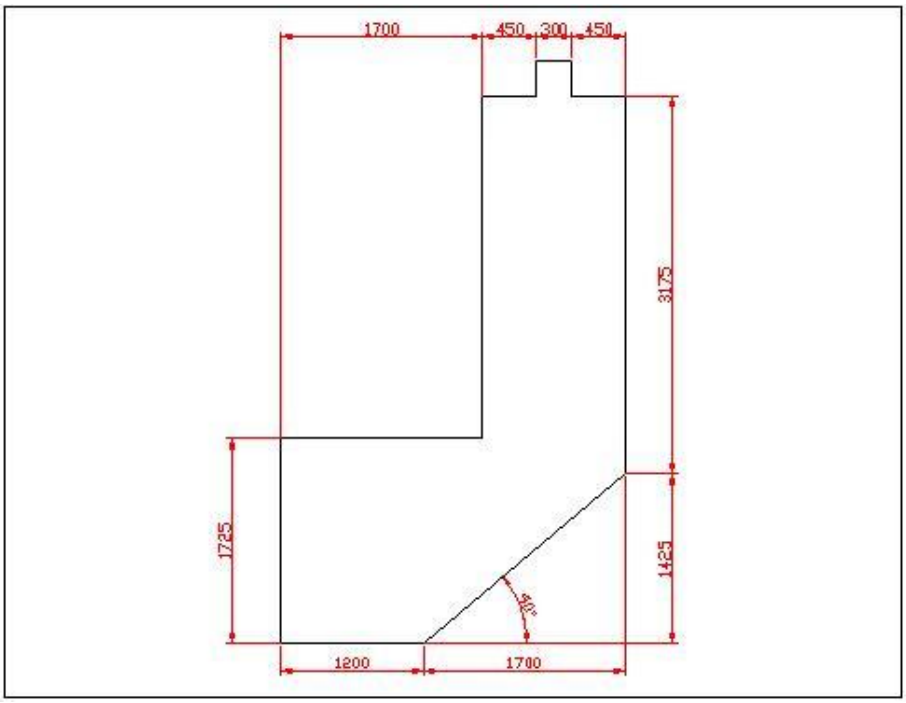

Figure 23: 2-D drawing of the design4

6) Design5 - Use 2 angle of inclined (40^{o})

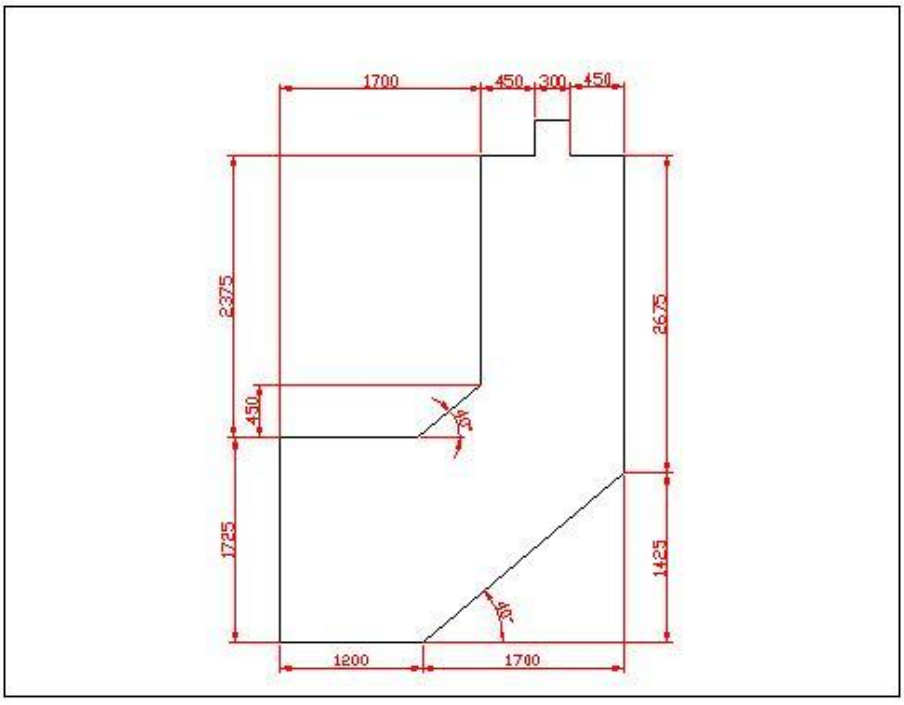

Figure 24: 2-D drawing of the design5

7) Design6 - Use 2 angle of inclined (60^o)

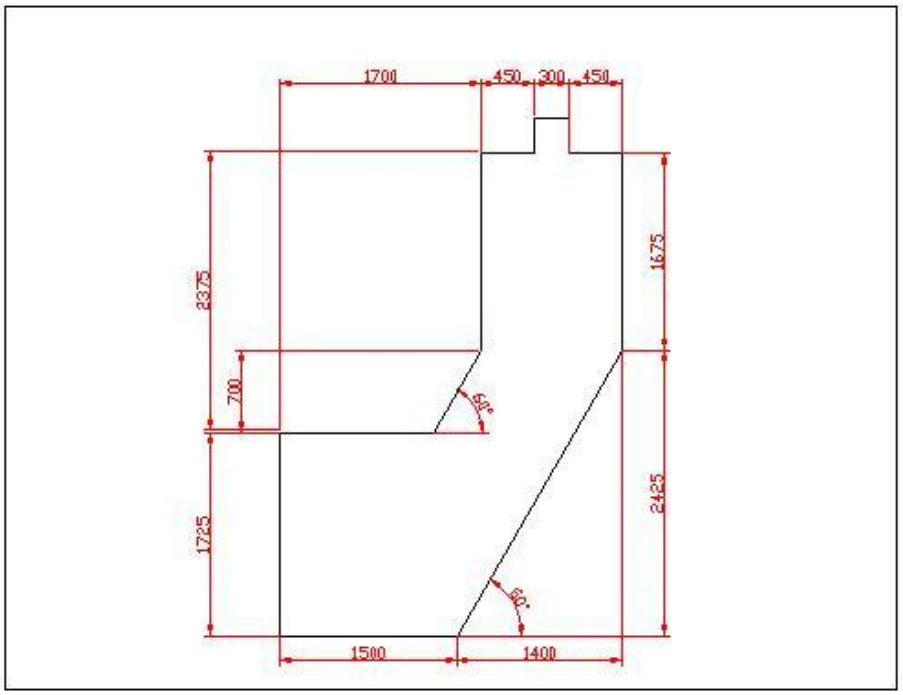

Figure 25: 2-D drawing of the design6

8) Design7 - Angle inclination changed to arc radius (1700*mm* radius)

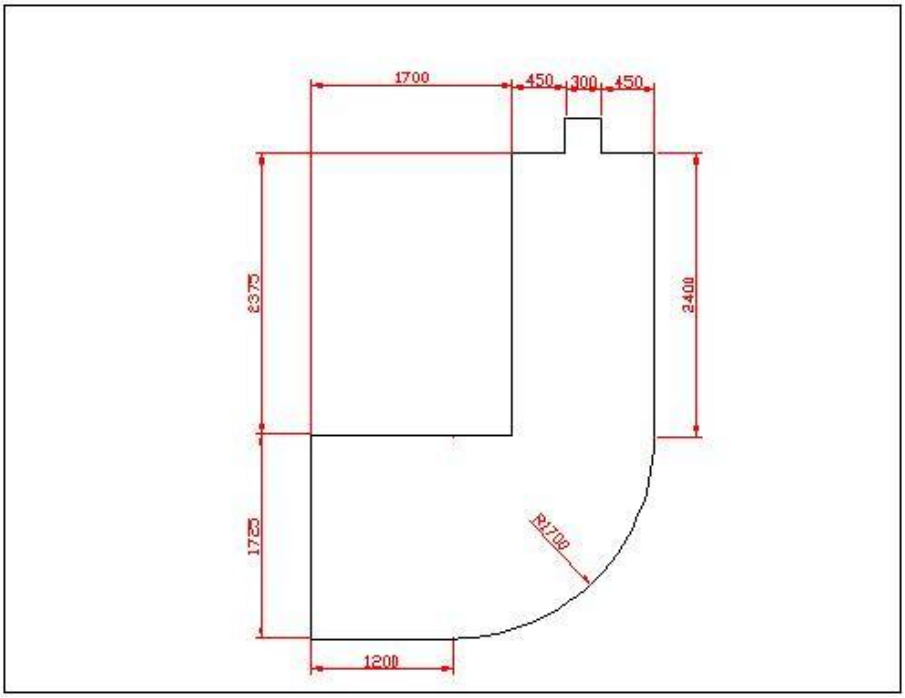

Figure 26: 2-D drawing of the design7

9) Design8 - Angle inclination changed to arc radius (2200*mm* radius)

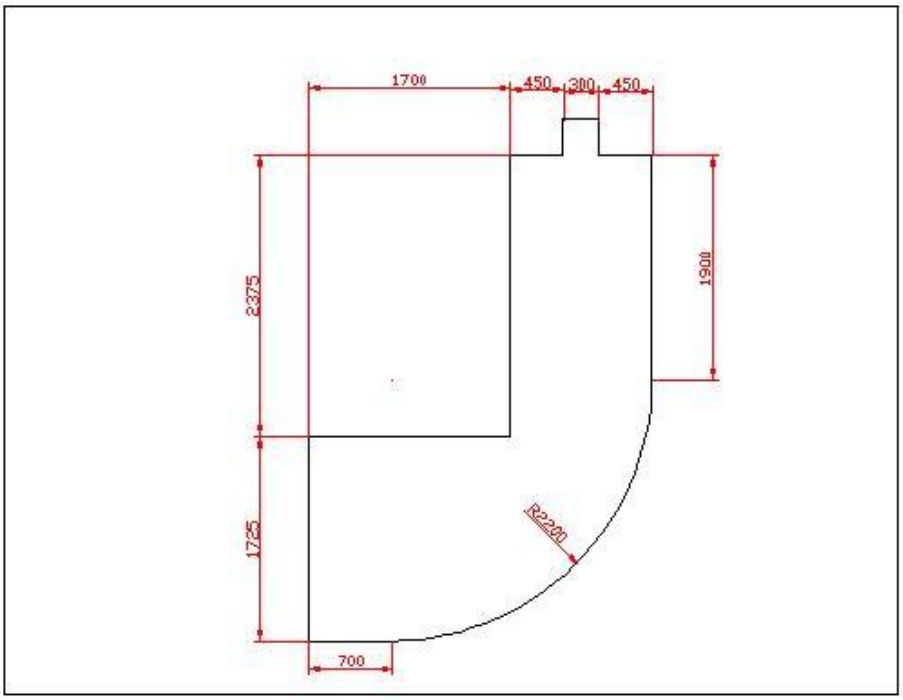

Figure 27: 2-D drawing of the design8

10) Design9 - Use 2arc radius (700*mm* and 1700*mm* radius)

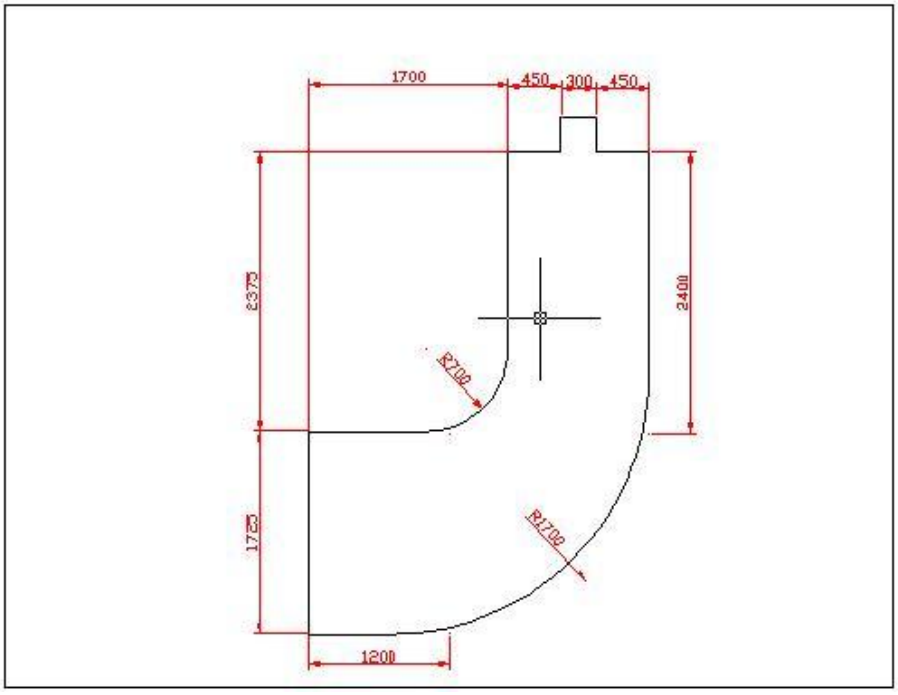

Figure 28: 2-D drawing of the design9

11) Design10 - Similar to design 5, but with horizontal outlet

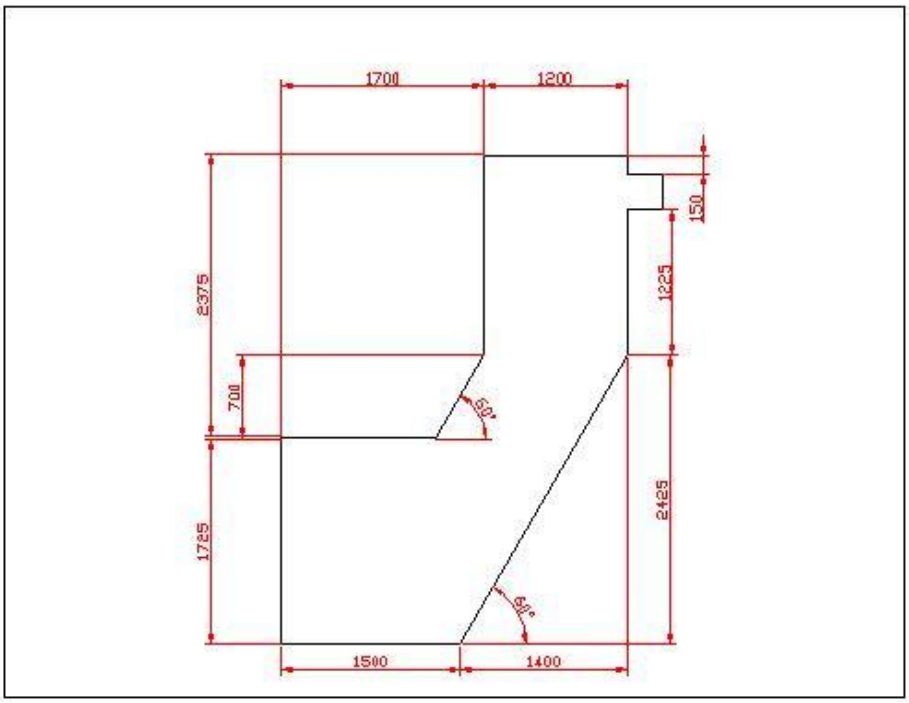

Figure 29: 2-D drawing of the design10

12) Design11 - Similar to design 6, but with horizontal outlet

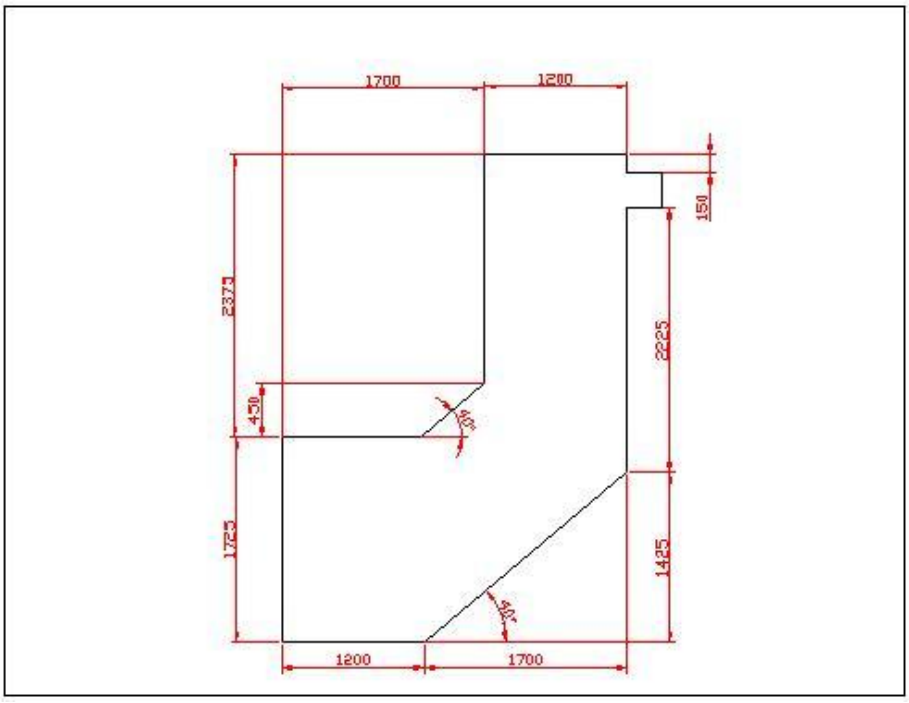

Figure 30: 2-D drawing of the design11

APPENDIX E - Contours of dynamic pressure and velocity magnitude (mixture) at 1000 iterations (0.5s flow) for each design

1) Design1

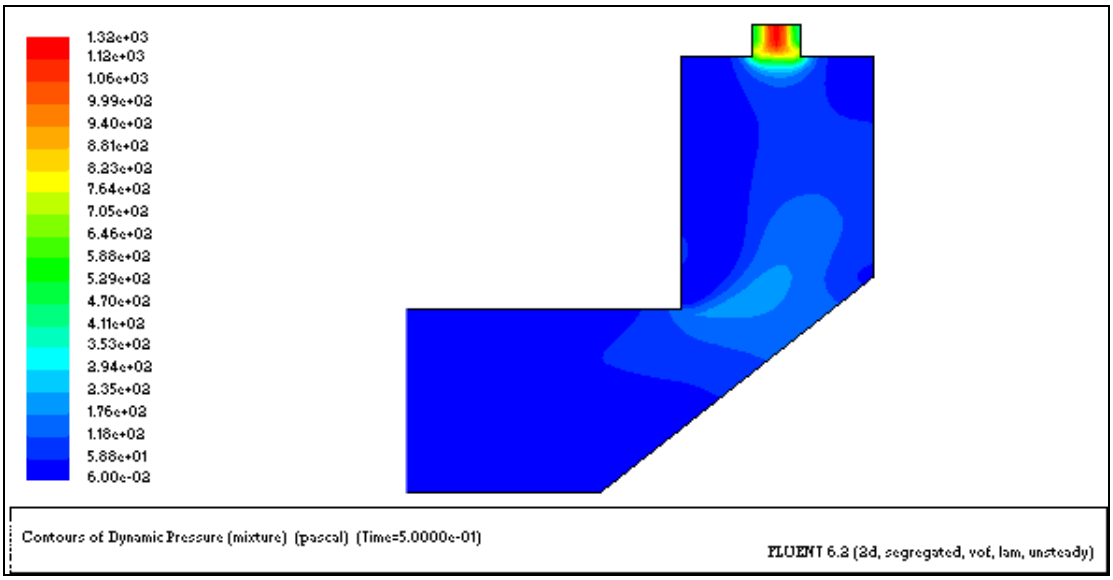

Figure 31: Contours of dynamic pressure (mixture) of Design1 (0.5s flow)

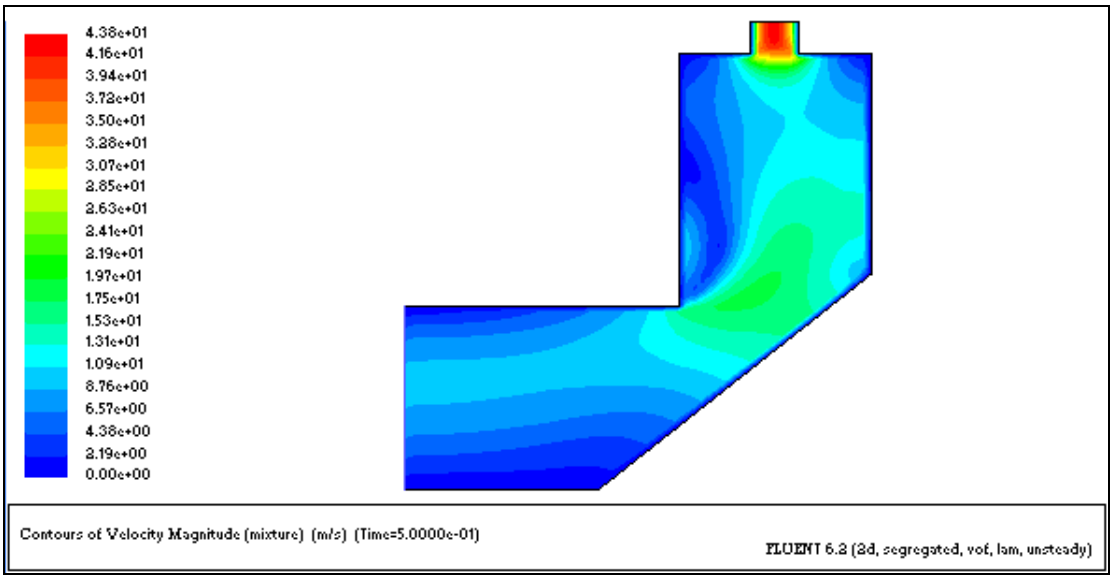

Figure 32: Contours of velocity magnitude (mixture) of Design1 (0.5s flow)

2) Design2

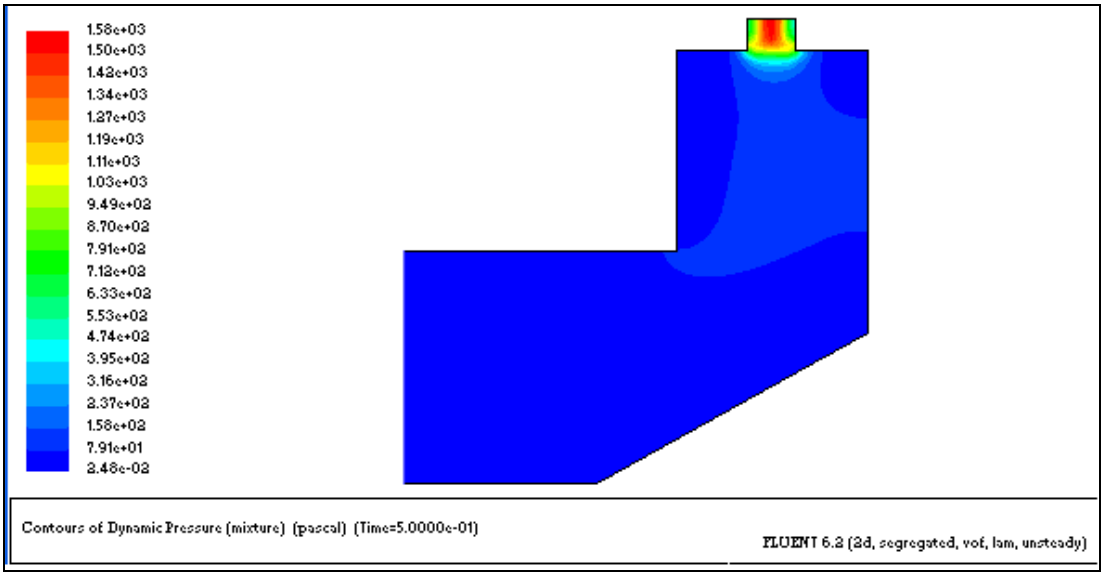

Figure 33: Contours of dynamic pressure (mixture) of Design2 (0.5s flow)

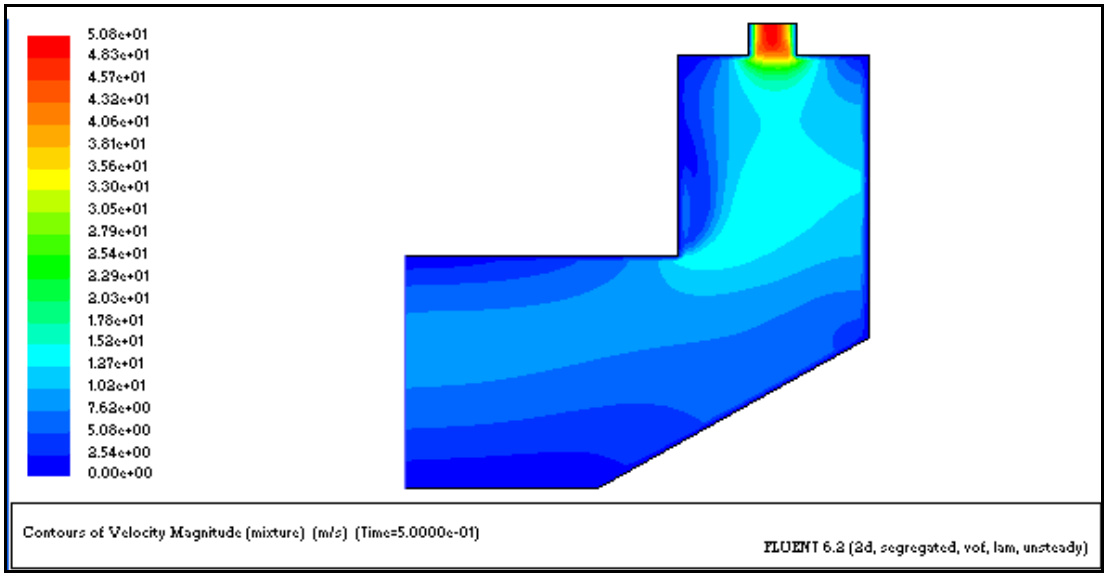

Figure 34: Contours of velocity magnitude (mixture) of Design2 (0.5s flow)

3) Design3

Figure 35: Contours of dynamic pressure (mixture) of Design3 (0.5s flow)

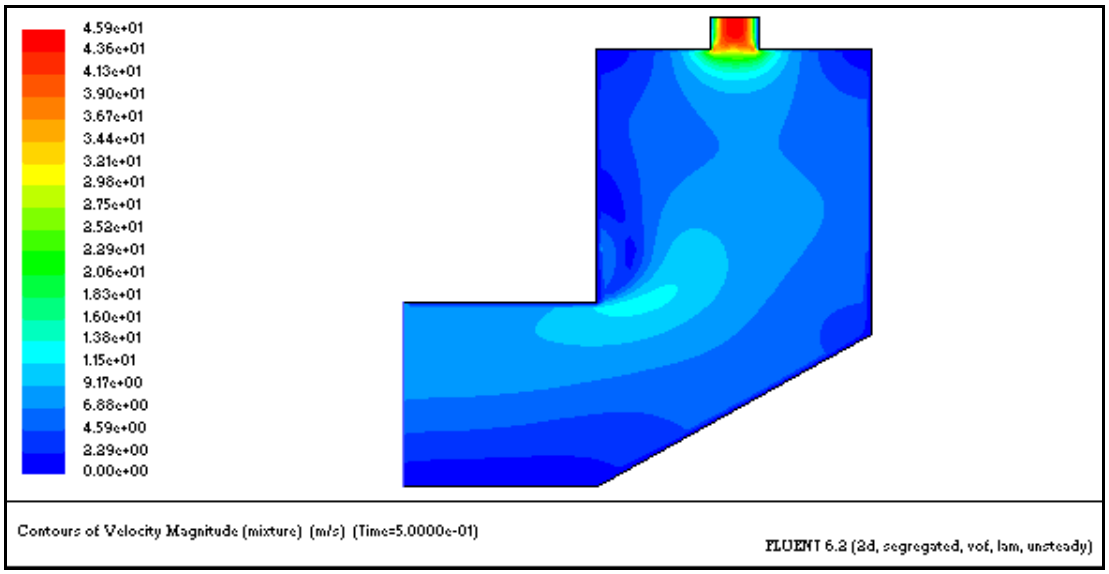

Figure 36: Contours of velocity magnitude (mixture) of Design3 (0.5s flow)

4) Design4

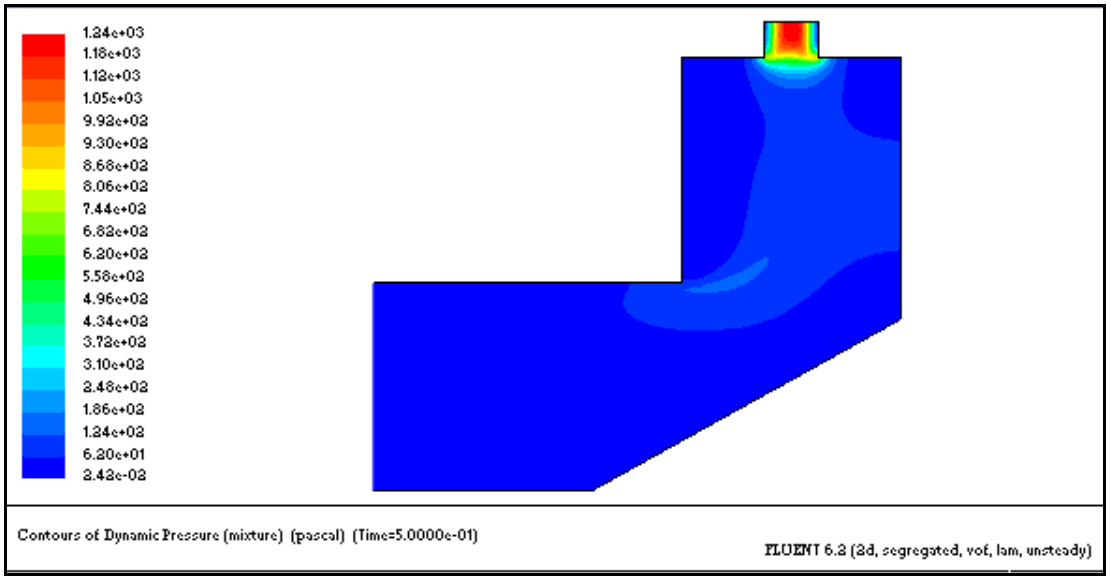

Figure 37: Contours of dynamic pressure (mixture) of Design4 (0.5s flow)

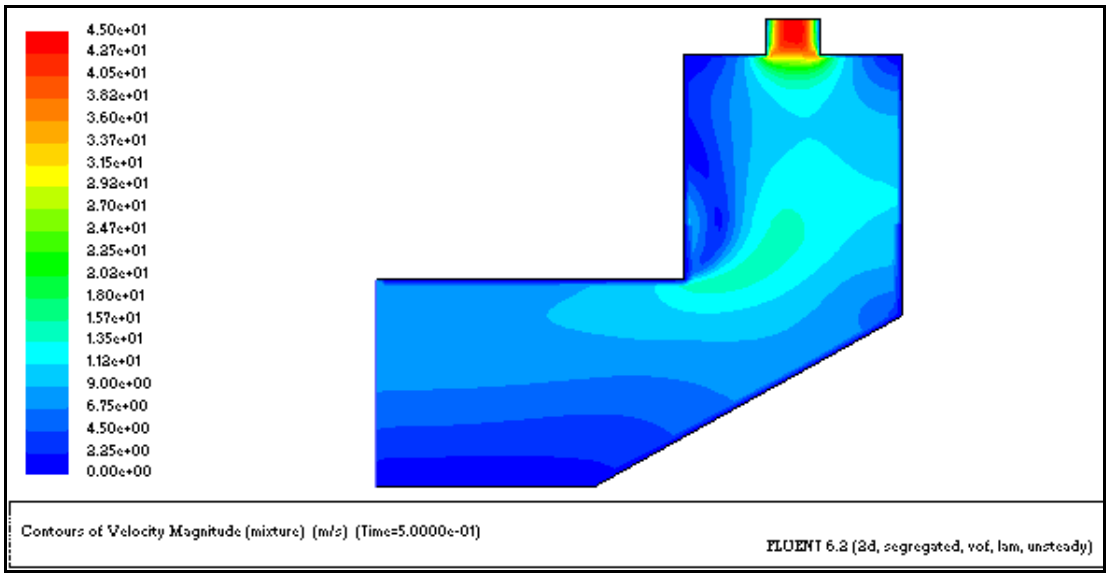

Figure 38: Contours of velocity magnitude (mixture) of Design4 (0.5s flow)

5) Design5

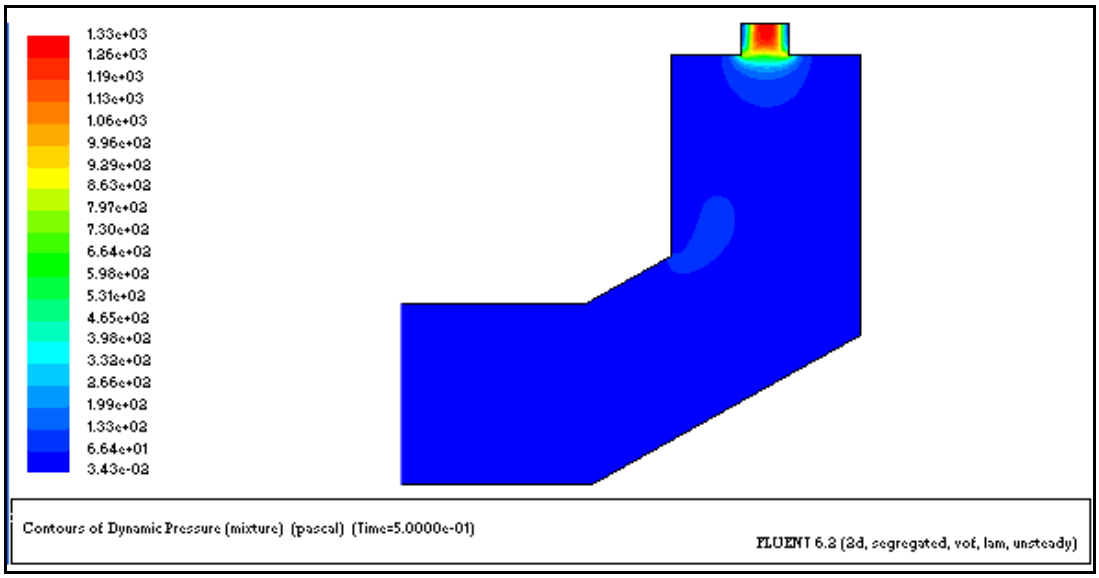

Figure 39: Contours of dynamic pressure (mixture) of Design5 (0.5s flow)

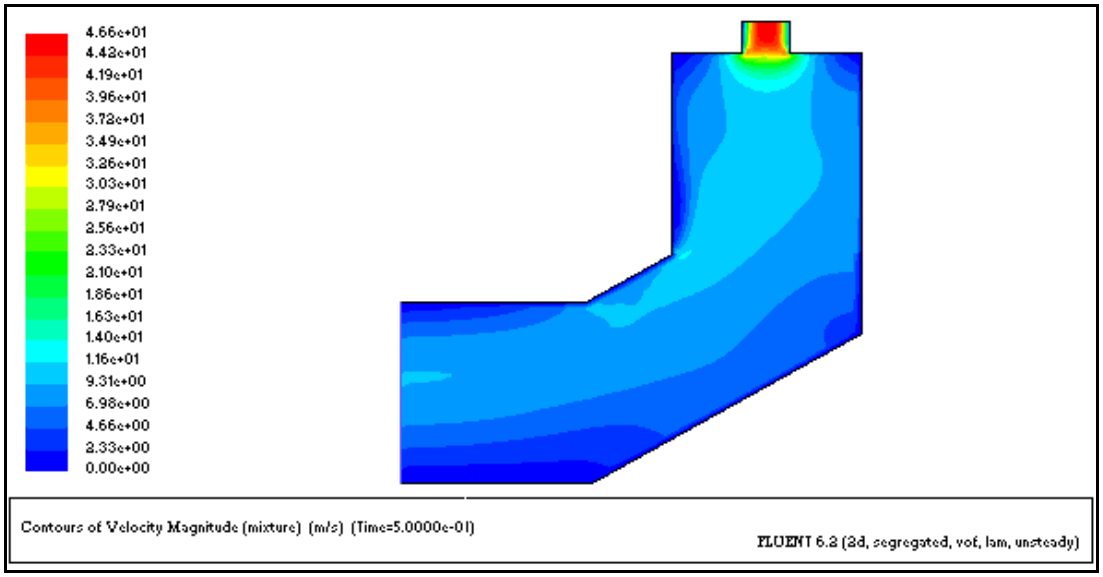

Figure 40: Contours of velocity magnitude (mixture) of Design5 (0.5s flow)

6) Design6

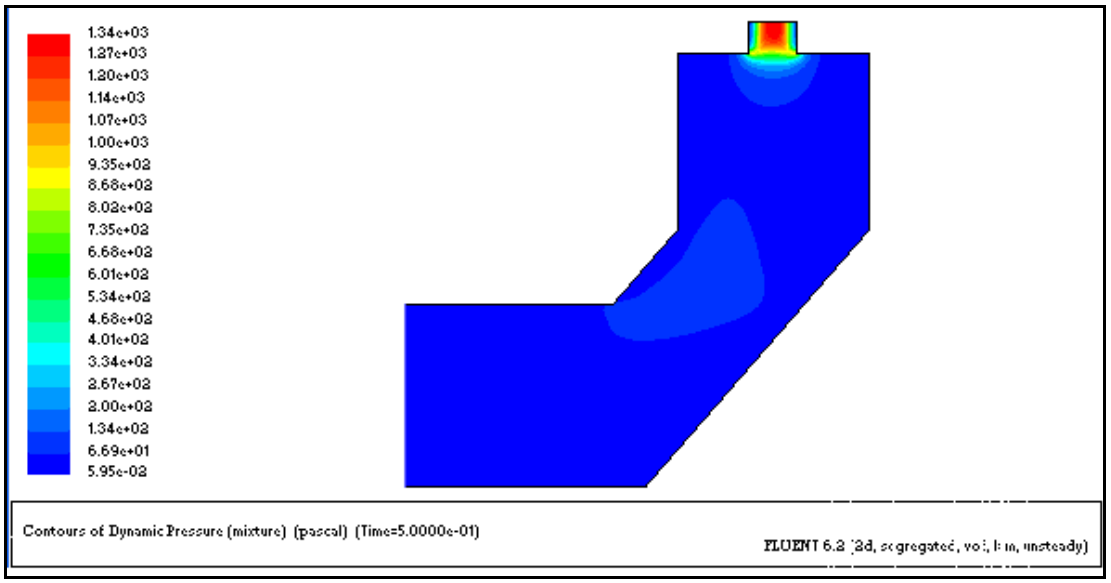

Figure 41: Contours of dynamic pressure (mixture) of Design6 (0.5s flow)

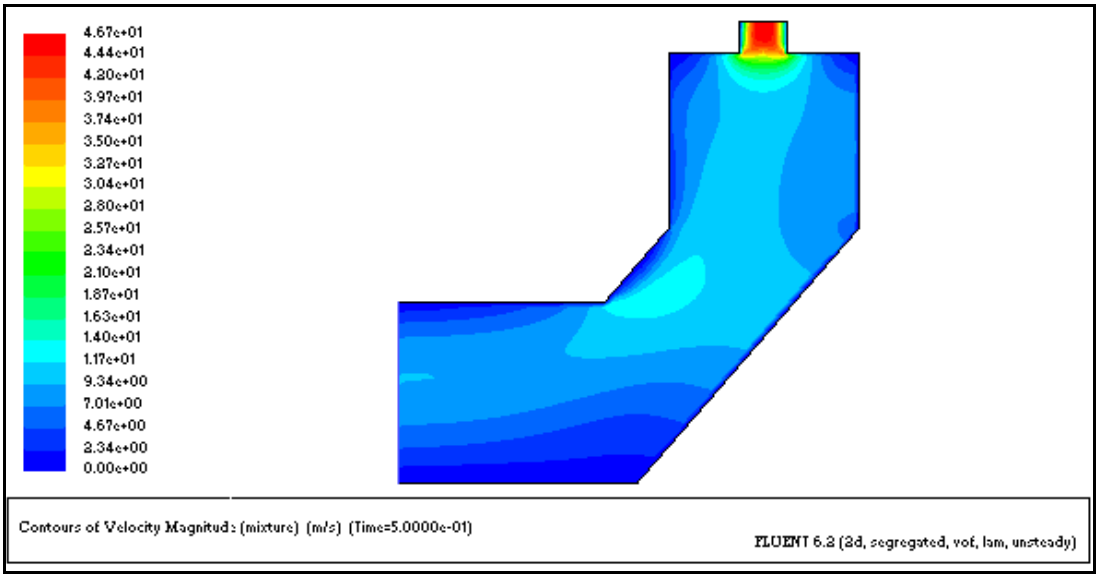

Figure 42: Contours of velocity magnitude (mixture) of Design6 (0.5s flow)

7) Design7

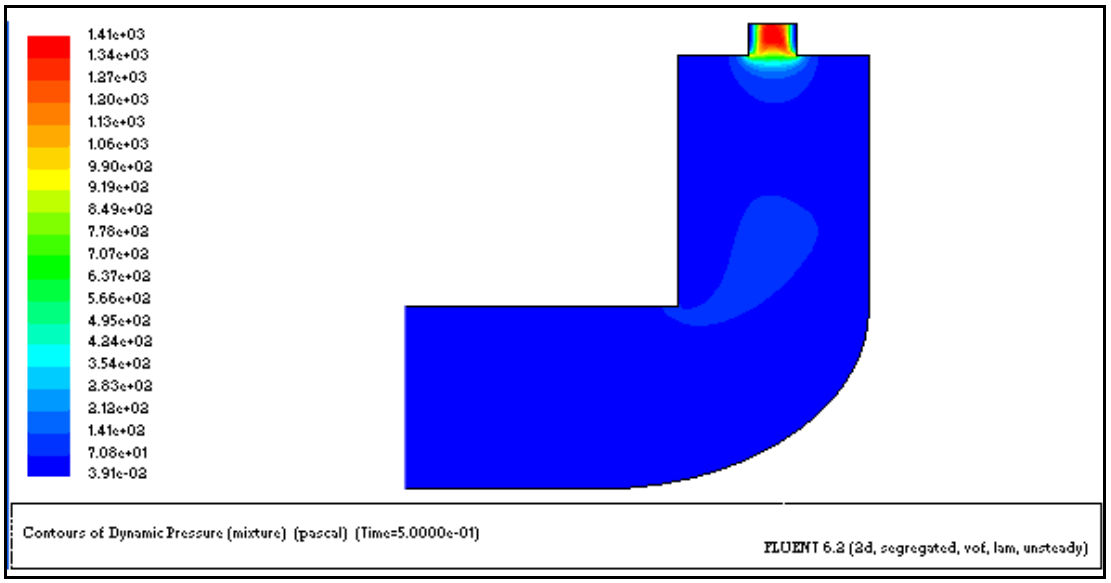

Figure 43: Contours of dynamic pressure (mixture) of Design7 (0.5s flow)

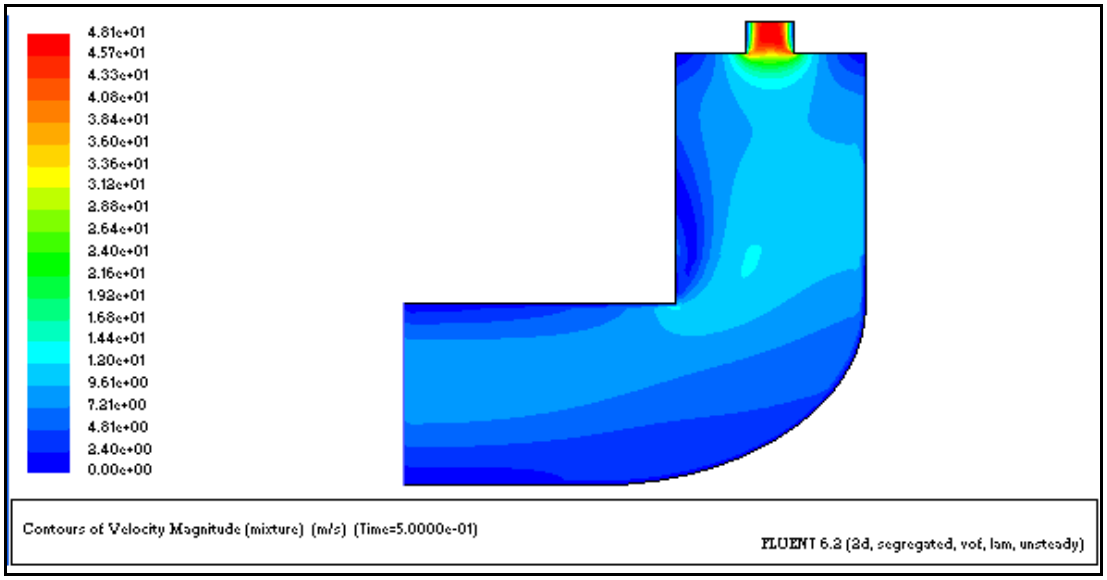

Figure 44: Contours of velocity magnitude (mixture) of Design7 (0.5s flow)

8) Design8

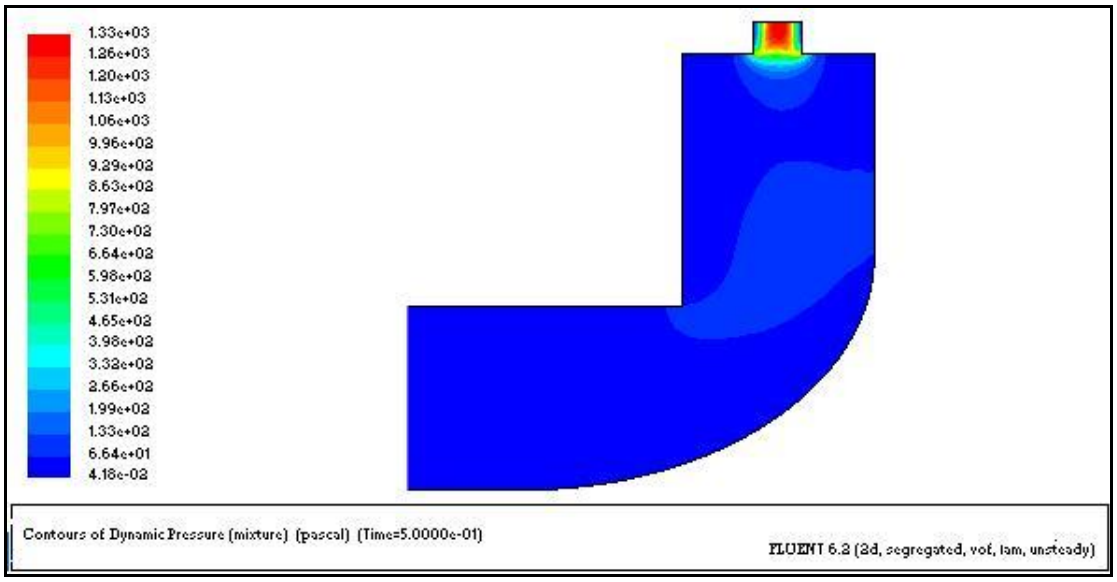

Figure 45: Contours of dynamic pressure (mixture) of Design8 (0.5s flow)

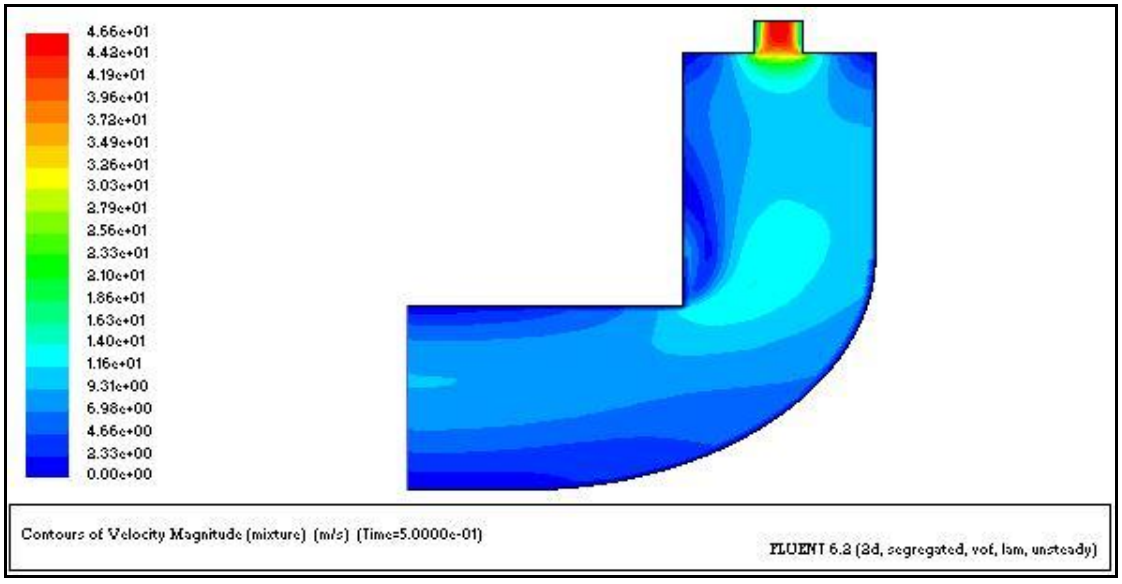

Figure 46: Contours of velocity magnitude (mixture) of Design8 (0.5s flow)

9) Design9

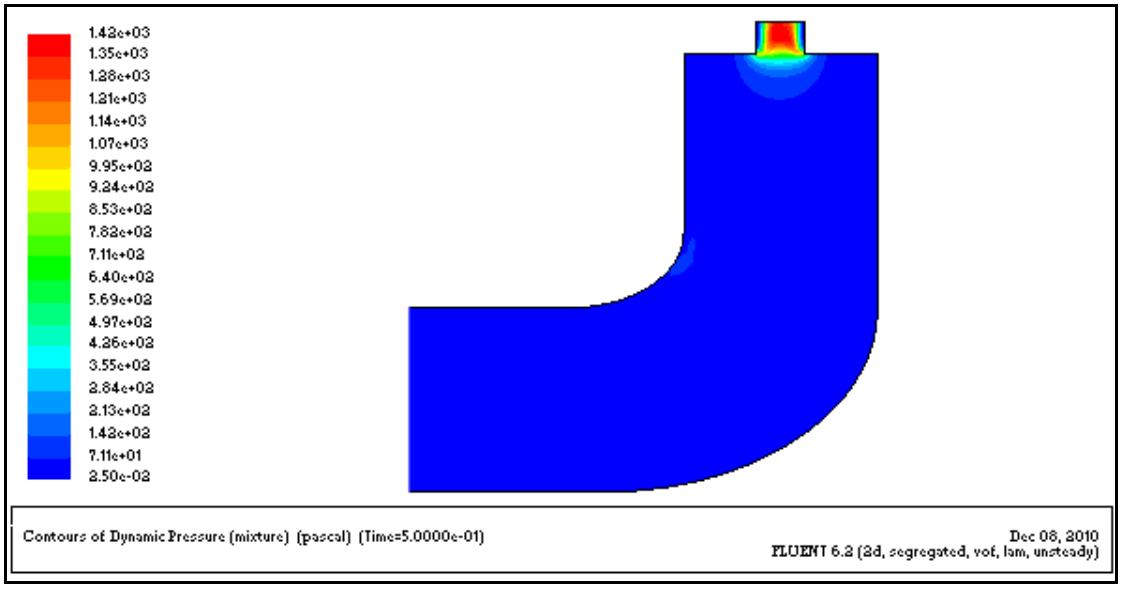

Figure 47: Contours of dynamic pressure (mixture) of Design9 (0.5s flow)

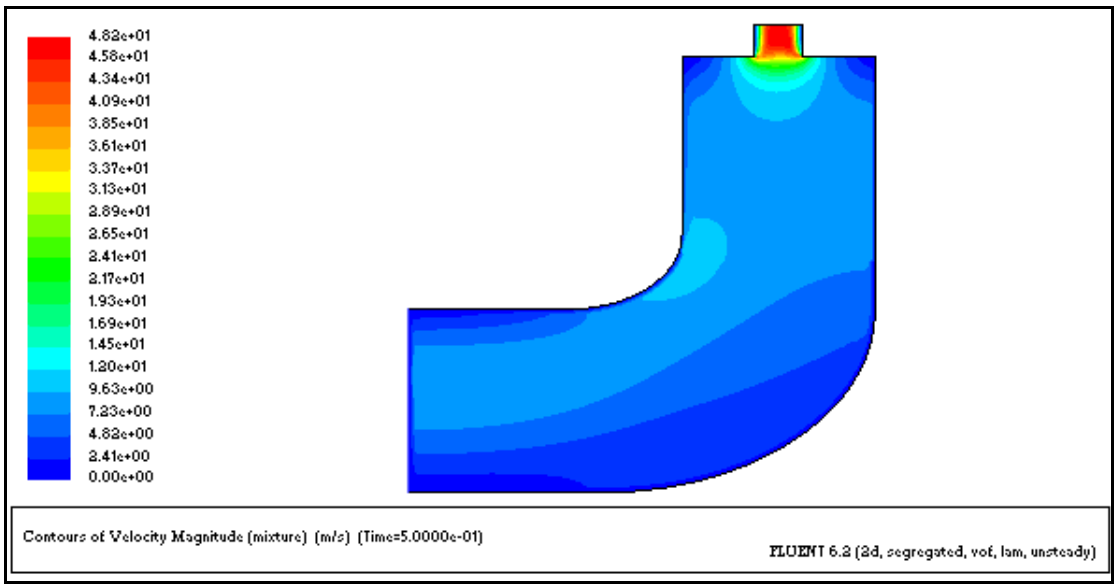

Figure 48: Contours of velocity magnitude (mixture) of Design9 (0.5s flow)

10) Design10

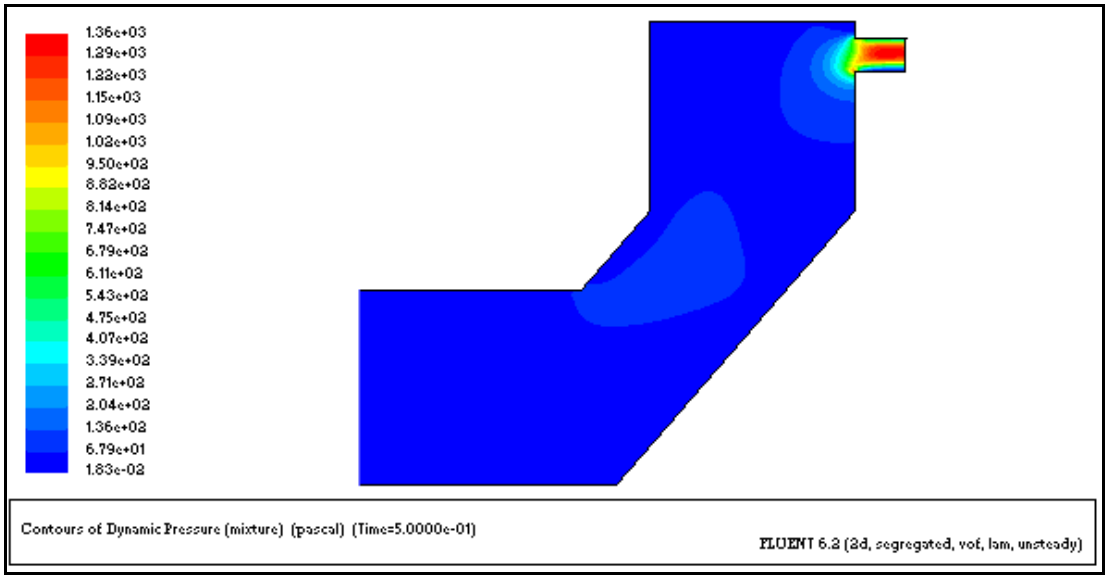

Figure 49: Contours of dynamic pressure (mixture) of Design10 (0.5s flow)

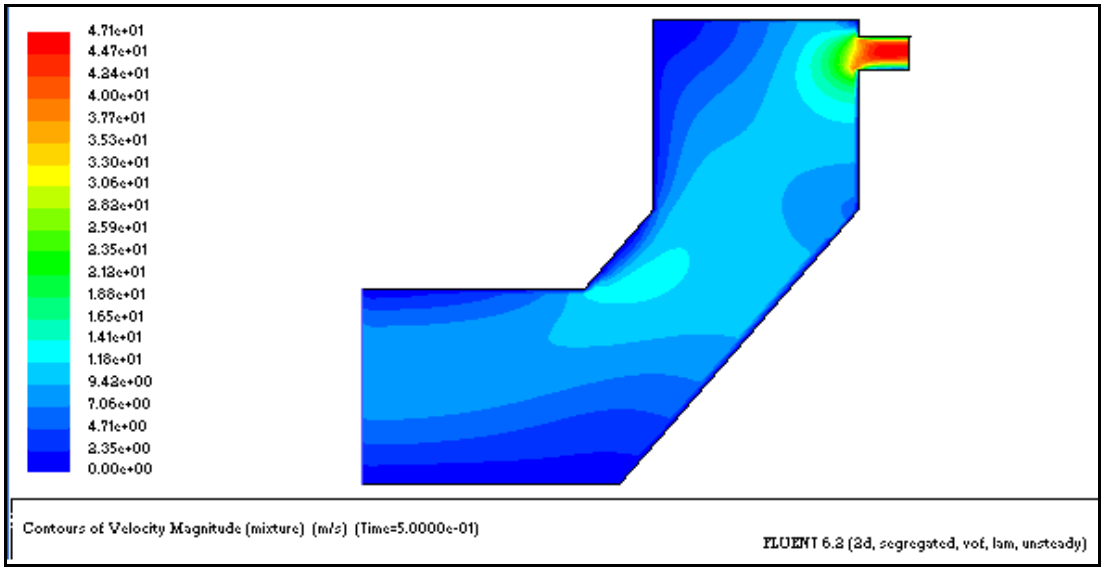

Figure 50: Contours of velocity magnitude (mixture) of Design10 (0.5s flow)

11) Design11

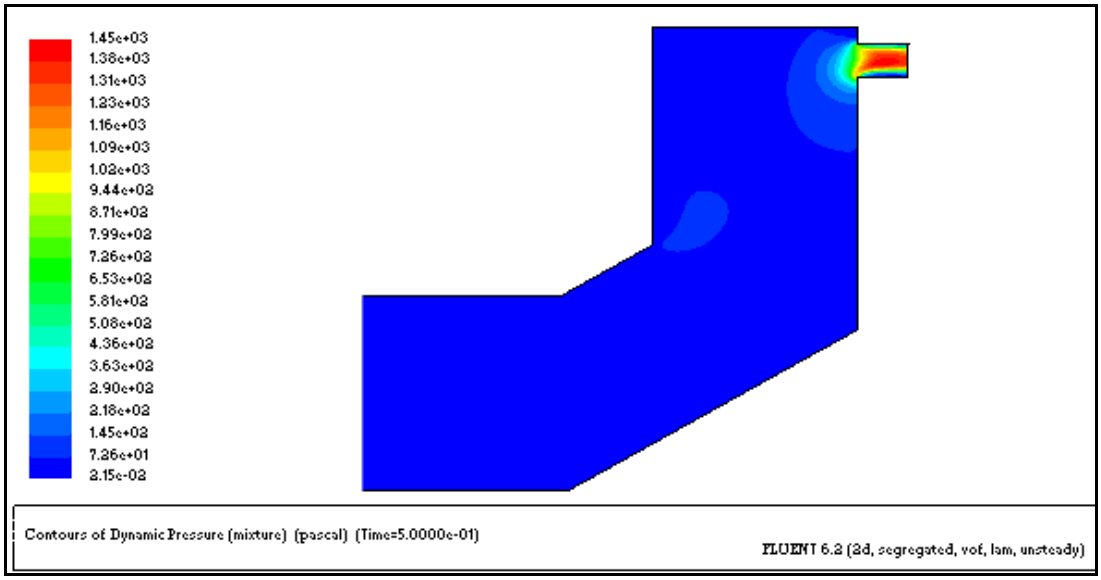

Figure 51: Contours of dynamic pressure (mixture) of Design11 (0.5s flow)

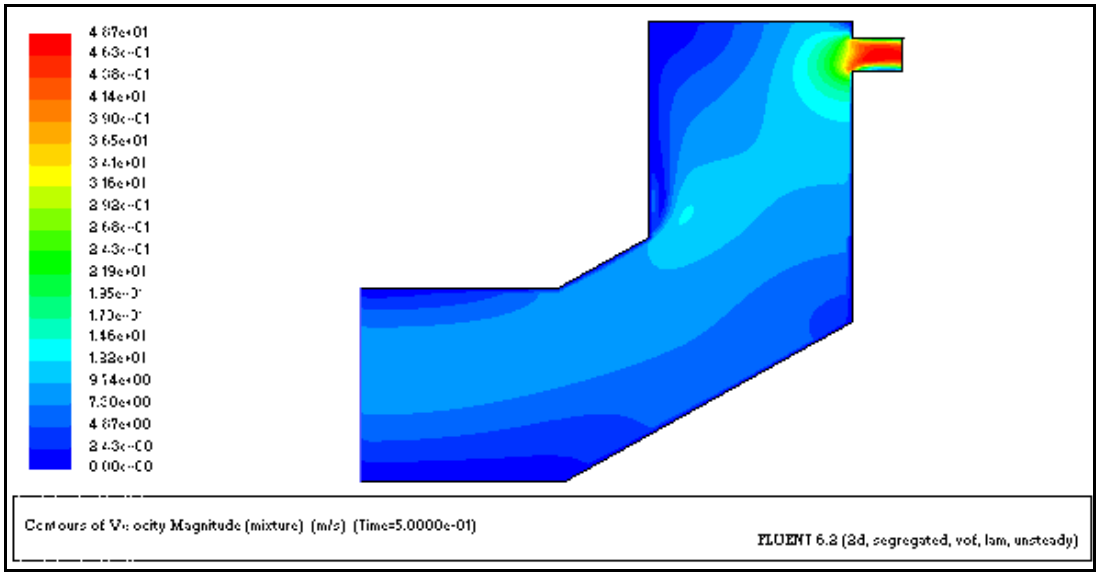

Figure 52: Contours of velocity magnitude (mixture) of Design11 (0.5s flow)